

Effects of enhancing nitrogen use efficiency in cropland and livestock systems on agricultural ammonia emissions and particulate matter air quality in China

Biao Luo<sup>1</sup>, Lei Liu<sup>2,3</sup>, David H. Y. Yung<sup>1</sup>, Tiangang Yuan<sup>1</sup>, Jingwei Zhang<sup>1</sup>, Leo T. H. Ng<sup>1</sup>, and Amos P. K. Tai<sup>1,4</sup>

<sup>1</sup>Department of Earth and Environmental Sciences, Faculty of Science, The Chinese University of Hong Kong, Sha Tin, Hong Kong, China

<sup>2</sup>State Key Laboratory of Lake and Watershed Science for Water Security, Nanjing Institute of Geography and Limnology, Chinese Academy of Sciences, Nanjing 211135, China

<sup>3</sup>College of Earth and Environmental Sciences, Lanzhou University, Lanzhou, Gansu, China

<sup>4</sup>State Key Laboratory of Agrobiotechnology, and Institute of Environment, Energy and Sustainability, The Chinese University of Hong Kong, Sha Tin, Hong Kong, China  
Correspondence to: Amos P. K. Tai (amostai@cuhk.edu.hk)

Abstract

Chinese agriculture has long been characterized by low nitrogen use efficiency (NUE) associated with substantial ammonia (NH<sub>3</sub>) loss, which contributes significantly to fine particulate matter (PM<sub>2.5</sub>) pollution. However, the knowledge gaps in the spatiotemporal patterns of NH<sub>3</sub> emissions and the states of nitrogen management of agricultural systems render it challenging to evaluate the effectiveness of different mitigation strategies and policies. Here, we explored the NH<sub>3</sub> mitigation potential of various agricultural NUE-improving scenarios and their subsequent effects on PM<sub>2.5</sub> pollution in China. We developed and used a combination of bottom-up emission models and a nitrogen mass flow model to evaluate the NUE of different crop and livestock types at a provincial scale in China. We generated gridded NH<sub>3</sub> emission input to drive a chemical transport model to provide an integrated assessment of the air quality impacts of four improved nitrogen management scenarios. The total agricultural NH<sub>3</sub> emission of China was estimated to be 11.2 Tg NH<sub>3</sub> in 2017, of which 46.2 % and 53.8 % are attributable to fertilizer use and livestock animal waste, respectively. Our results show that grain crops have higher NUE than fruits and vegetables, while high livestock NUE can be found in pork and poultry. We also found that by implementing different mitigation scenarios, agricultural NH<sub>3</sub> emissions can be effectively reduced by 11.6%–39.3%. Consequently, annual population-weighted PM<sub>2.5</sub> reductions were estimated to be 1.3–4.1 μg m<sup>-3</sup>. Our results provide decision support for policymaking concerning agricultural NH<sub>3</sub> emissions and their public health impacts.

1. Introduction

High nitrogen (N) input in croplands is the key to meeting the increasing food demand in China, but it also simultaneously poses severe burdens to the environment, damaging ecosystem and human health (Guo et al., 2020). China’s grain production

删除了： State Key Laboratory of Nutrient Use and Management, Beijing Key Laboratory of Farmland Soil Pollution Prevention and Remediation, College of Resources and Environmental Sciences, National Academy of Agriculture Green Development, China Agricultural University, Beijing, China

nearly doubled from 1980 to 2017, while N synthetic fertilizer use more than tripled during the same period (NBSC, 2023).

Large N surplus in croplands, which cannot be stored in soil or absorbed by the crops in a timely manner, inevitably causes massive reactive N leakage to the environment. The situation regarding livestock production is also concerning. Population growth and dietary changes have led to a substantial increase in meat consumption in China, rising from 13.4 Mt in 1980 to 77.3 Mt in 2010 (Liu et al., 2021), which has expanded China's livestock population accompanied by substantial amounts of excretion and animal waste with rich N content. Improper manure handling and poor management result in only 30% of N excretion being recycled to farmlands, with the rest being released to the environment (Zhang et al., 2023).

Among these reactive N losses, ammonia ( $\text{NH}_3$ ) emissions have become an increasing concern for the Chinese government in recent years.  $\text{NH}_3$ , primarily emitted from agricultural activities, plays essential roles in ecosystems, atmosphere chemistry, and climate (Li et al., 2021; Zhang et al., 2018). It can react with sulfuric acid ( $\text{H}_2\text{SO}_4$ ) and nitric acid ( $\text{HNO}_3$ ) produced from the oxidation of sulfur dioxide ( $\text{SO}_2$ ) and nitrogen oxides ( $\text{NO}_x \equiv \text{NO} + \text{NO}_2$ ), respectively, and contribute to the formation of sulfate-nitrate-ammonium (SNA) aerosols (Behera et al., 2013). Ammonium aerosols exhibit well-documented effects on climate, with their ability to scatter sunlight and act as cloud condensation nuclei to promote cloud formation (Abbatt et al., 2006; Henze et al., 2012). Additionally, it can increase fine particulate matter ( $\text{PM}_{2.5}$ , i.e., particulate matter with a diameter of  $2.5 \mu\text{m}$  or smaller) pollution, a severe public health concern worldwide. China is a global hotspot of  $\text{NH}_3$  emissions, accounting for 25% of global emissions (Liu et al., 2022). Agricultural  $\text{NH}_3$  emissions, driven by low nitrogen use efficiency (NUE) in Chinese agriculture, account for over 80% of  $\text{NH}_3$  emissions in China, contributing to around 16% of the  $\text{PM}_{2.5}$  mass burden in China (Han et al., 2020).

Due to China's aggressive clean air actions in recent years,  $\text{SO}_2$  and  $\text{NO}_x$  emissions have been reduced significantly.  $\text{NH}_3$  was not initially listed in the clean air actions. However, there is growing evidence of the importance of  $\text{NH}_3$  for  $\text{PM}_{2.5}$  control in China. Fu et al. (2017) indicated that the rise in  $\text{NH}_3$  concentrations has undermined the benefits of reducing SNA concentrations (especially for nitrate) via emissions control of  $\text{SO}_2$  and  $\text{NO}_x$ . Comparing air pollution in China before and after the COVID-19 lockdown, Xu et al. (2022) observed that while there was a sharp reduction in  $\text{SO}_2$  and  $\text{NO}_x$  emissions during the lockdown, the concurrent increase in  $\text{NH}_3$  concentrations may have contributed to the persistent high levels of  $\text{PM}_{2.5}$  pollution. Therefore, the Chinese government has recently recognized the significance of  $\text{NH}_3$  emissions in controlling  $\text{PM}_{2.5}$  pollution and included them in the list of regulated atmospheric pollutants.

With improving technology and management of agricultural production, some abatement pathways are available for controlling  $\text{NH}_3$  emissions. For fertilizer-related  $\text{NH}_3$ , deep placement of fertilizer, optimization of fertilizer schedules, enhanced-efficiency fertilizers (e.g., controlled-release fertilizer), and adding nitrification and urease inhibitors are all effective options, with mitigation efficiency range between 14–87 % (Fu et al., 2020; Huang et al., 2016; Liu et al., 2021; Ren et al.,

2022). As for  $\text{NH}_3$  loss from livestock waste, one may improve feed management (e.g., low crude protein feeding) and utilize manure treatment technology such as rapid manure drying, solid-liquid separation, and composting during housing and storage stages, and the reported mitigation efficiency is 10–55 % (Bai et al., 2016; Hou et al., 2015; Zhang et al., 2020). In addition, the recycling of manure nutrients to farmlands as a substitute for synthetic fertilizers is an important approach to decrease emissions. Undoubtedly, these efforts can enhance NUE of Chinese agricultural systems. To link the above measures with mitigation potential analysis, the emission reduction efficiencies of various control options derived from meta-analysis have been applied to regional and national scales to explore the emission mitigation potential (Fu et al., 2020; Guo et al., 2020). This, however, assumes that regions have the same status of nitrogen use and the various technologies will deliver the expected outcomes. Moreover, some studies have attempted to evaluate the current agricultural NUE and identify the emission reduction potential by closing the gap between the current and optimal NUE (Bai et al., 2016; Zhang et al., 2020). Such studies, however, usually focused only on national and entire crop or livestock systems, making it challenging to identify specific recommendations for different crops in different regions.

An accurate and detailed  $\text{NH}_3$  emission inventory is the basis for mitigation potential evaluation. High-resolution gridded agricultural  $\text{NH}_3$  emission inventory can not only quantify the contribution of different sectors but also show the precise spatiotemporal patterns of emissions, which can further serve as input of air quality models to investigate their impacts on air quality and human health. Bottom-up estimation is the primary approach to establishing  $\text{NH}_3$  emission inventories (Battye et al., 2003; Huang et al., 2012; Meng et al., 2017). Many studies have generated regional and global agricultural  $\text{NH}_3$  emission inventories via this approach, such as EDGAR, REAS, CEDS, PKU- $\text{NH}_3$ , and MEIC (Crippa et al., 2020; Kurokawa and Ohara, 2020; McDuffie et al., 2020; Kang et al., 2016; Li et al., 2017). The common way to produce a gridded inventory has two steps: (1) estimating the total  $\text{NH}_3$  emission at the administrative unit (e.g., country, province, and county scale) via activity data (mainly from census) and emission factors (EFs); (2) allocating emissions to grid cells based on different base-maps (e.g., population density, crop and livestock distribution). The spatial accuracy of an inventory is decided by the resolution of the base-maps. High-resolution inventories (e.g., ~1 km) are usually gridded based on land use and population density map (~1 km), without any crop or livestock spatial information (Huang et al., 2012; Kang et al., 2016). On the other hand, inventories at a coarser resolution (e.g., ~10 km) consider livestock and crop distribution, but are constrained by the spatial resolution of available crop and livestock data (Yang et al., 2023; Zhang et al., 2018).

This study aims to evaluate the NUE and  $\text{NH}_3$  emissions of the agricultural systems of China in 2017, and further investigate the various potentials of reducing  $\text{NH}_3$  emissions and their subsequent effects on  $\text{PM}_{2.5}$  pollution. The objectives are to: (1) develop a high-resolution agricultural  $\text{NH}_3$  inventory (1 km), including 16 crop types and six livestock types, based on a newly available crop and livestock distribution map; (2) evaluate the NUE of six crop subsystems and four livestock

subsystems; (3) design four prospective mitigation scenarios, consisting of enhancing NUE of crops and livestock, improving organic fertilizer use ratio, and combined measures; (4) calculate NH<sub>3</sub> emission reductions and benefits in terms of air quality enhancements under these mitigation scenarios based on a chemical transport model. This study provides useful insights into how further decreasing NH<sub>3</sub> emissions toward cleaner air goals can be achieved by improving the NUE of agricultural systems in China.

## 2. Materials and methods

### 2.1. Bottom-up estimates of agricultural emissions

In this study, we estimated agricultural NH<sub>3</sub> emissions as a function of agricultural activity data and EFs, which is an approach widely applied in previous bottom-up estimation (Zhan et al., 2021; Bouwman et al., 2002; Paulot et al., 2014). We chose 2017 as the baseline for our study. The rationale behind was that the African swine fever in China significantly impacted pork production between 2018 and 2021, resulting in the death of over a million pigs (Liu & Zheng, 2024), and the COVID-19 pandemic also influenced agriculture substantially between 2019 and 2022. Therefore, after excluding these impacts, 2017 is the closest “present-day” representative year with complete data. The NH<sub>3</sub> emission ( $E_i$ , kg NH<sub>3</sub>) from a given source  $i$  is calculated as:

$$E_i = A_i \times EF_i \quad (1)$$

where  $A_i$  is activity data of source  $i$ , such as the total synthetic fertilizer use for crops and the livestock population;  $EF_i$  is the emission factor of source  $i$ , which could be derived from functions of environmental conditions, management, and source types.

#### 2.1.1. Fertilizer-related NH<sub>3</sub> emissions

The total fertilizer application is determined by the crop planting structure and fertilizer application rates, which have significant spatiotemporal variability. Because of uncertainties in the timing of fertilizer application, we employed the Gaussian distribution function (Eq. 2) to quantify variations in fertilizer application (Gyldenkerne et al., 2005; Paulot et al., 2014).

$$F_{ct} = R_c \times \frac{1}{\delta_c \sqrt{2\pi}} \times e^{-\frac{(t-\mu_c)^2}{2\delta_c^2}} \times PA_c \quad (2)$$

where  $c$  stands for different crops and  $t$  represents month;  $F_{ct}$  (kg) is the total fertilizer use of crop  $c$  at month  $t$ ;  $R_c$  (kg ha<sup>-1</sup>) is the fertilizer application rate of crop  $c$ ;  $\mu_c$  is the fertilizer application time crop  $c$ ;  $\delta_c$  is the deviation from the mean planting date crop  $c$  (Sacks et al., 2010);  $PA_c$  (ha) is the crop planting areas crop  $c$ .

The fertilization of vegetables and fruits is assumed to be the same for every month. Functions of soil properties, fertilizer application, and crop planting information are used to calculate the baseline EF (Eq. 3):

$$EF_0 = e^{f(\text{pH})+f(\text{CEC})+f(\text{crop})+f(\text{fertilizer type})+f(\text{application mode})} \quad (3)$$

where  $f$  is a function that accounts for the effect of soil pH, cation exchange capacity (CEC), fertilizer type, and application mode on EF of fertilizer application. The functions were obtained from previous results for China (Huang et al., 2012; Kang et al., 2016; Zhang et al., 2018), which are summarized in the supplementary materials (Table S1 and S2). The gridded soil pH and CEC data (1 km × 1 km) were obtained from the Harmonized World Soil Database (<https://www.fao.org/land-water/databases-and-software/hwsd/en/>, last accessed: October 2023) (Fig. S1).

The baseline EF is further corrected by monthly meteorological factors (Eq. 4) (Paulot et al., 2014):

$$EF = EF_0 \times (e^{0.0223T_m + 0.0419u_m}) / \left( \frac{1}{12} \sum_{m=1}^{12} e^{0.0223T_m + 0.0419u_m} \right) \quad (4)$$

where  $m$  represents months;  $T$  (°C) and  $u$  (m s<sup>-1</sup>) are air temperature and wind speed at 2 m height, whereby their gridded values (1 km × 1 km) are from Peng et al. (2019) and National Earth System Science Data Center (<http://www.geodata.cn/>, last accessed: October 2023), respectively. The high-resolution climate data were produced by spatially downscaling the 30-min Climatic Research Unit (CRU) time-series dataset with WorldClim climatology using the delta downscaling method.

设置了格式：字体：非加粗

#### 2.1.2. NH<sub>3</sub> emissions from livestock manure

NH<sub>3</sub> emissions from livestock are closely related to livestock excretion and how manure is managed (Hou et al., 2015). There are three typical types of livestock raising patterns in China: intensive, free-range and grazing, and their manure management approaches are different (Huang et al., 2012). Following Huang et al. (2012) and Kang et al. (2016), we adopted a mass-flow approach by considering N flows in different stages. Total ammoniacal nitrogen (TAN) from livestock waste is estimated first, and then it flows into the manure management stages. NH<sub>3</sub> escape rate from manure varies in slurry vs. solid forms (housing, storage, and spread). The livestock excretion rates and EFs are obtained from Huang et al. (2012), which are shown in Table S3 and Table S4. The livestock EFs were first calculated for each livestock type across livestock manure management stages. Same as Zhang et al. (2018), these EFs are further modulated by the effect of temperature and wind speed following Eq. 4.

删除了：,

删除了：emissions

#### 2.1.3. Gridded emissions

Following the approach described above, we first calculated NH<sub>3</sub> emissions from fertilizer and livestock waste on a province scale. Here we estimated 16 crops of China in 2017, and the planting area and fertilizer application rates of each crop in each province were obtained from the National Bureau of Statistics of China (NBSC) (<http://www.stats.gov.cn/tjsj/>, last

155 accessed: October 2023). Six livestock types, including cattle, other big animals (e.g., horse, donkey, and camel), goat, sheep,  
 160 pork, and poultry, were considered. The livestock numbers at the end of the year and slaughter numbers for each province were  
 also from national statistics (<http://www.stats.gov.cn/tjsj/>, last accessed: October 2023). The provincial statistical data can be  
 found in Table S5 and S8. According to the above methods (section 2.1.1 and 2.1.2), the crop- and livestock-specific NH<sub>3</sub>  
 emissions of each province were estimated. Then, we gathered the spatial distribution of crop planting area, livestock  
 population, and cropland area. Due to a lack of high-resolution data of crop planting area, only rice, wheat, and maize gridded  
 data at 1 km resolution could be obtained from Luo et al. (2020) (Fig. S2). These three crops account for nearly 60 % of China's  
 total planting area, ensuring that we can reproduce most of the spatial patterns of fertilizer-related NH<sub>3</sub> emissions. It is assumed  
 that all other crops are distributed uniformly throughout the croplands of each province. The spatial distribution of cropland  
 area was provided by the Data Center for Resources and Environmental Sciences, Chinese Academy of Sciences (RESDC)  
 165 (<http://www.resdc.cn>, last accessed: October 2023) (Fig. S2). The gridded livestock population map at 1 km, including cattle,  
 sheep, goat, pork, and poultry was obtained from Cheng et al. (2023) (Fig. S3). The livestock map consolidates data from  
 various sources, encompassing provincial, municipal, and county statistics, alongside agricultural census records and intensive  
 farm registration data. Intensive livestock populations, constituting ~60% of the total livestock count, are assigned to 1 km  
 grid cells according to the positions and breeding scales of intensive livestock farms. Meanwhile, extensive livestock  
 170 populations, primarily comprised of backyard farms involving smallholders, are allocated based on the spatial distribution of  
 rural inhabitants. This dataset offers heightened precision compared to existing livestock distribution maps, particularly in  
 delineating livestock presence across urban, peri-urban, and rural regions.  
The maps of EFs were created for each grid cell using Eq. 3 and Eq. 4, first by calculating the baseline EFs first and  
 further modulating them by meteorological conditions. We then combined the spatial distribution of crop planting area,  
 175 cropland area, and livestock population with the EF maps to produce gridded NH<sub>3</sub> emission maps. Finally, the NH<sub>3</sub> emissions  
 of each province were used to correct gridded NH<sub>3</sub> emission maps so that when estimates in grid cells are summed over a  
 province the total would match the provincial total:

$$E_j = E_j^0 \times \frac{E_p}{\sum_j^p E_j^0} \quad (5)$$

180 where  $E_j$  (kg) is the emission flux in pixel  $j$ ;  $E_j^0$  (kg) represents the emission in pixel  $j$  without correction;  $E_p$  (kg) is the total  
 emission of province  $p$ ;  $\sum_j^p E_j^0$  stands for the sum of emissions over all pixels in province  $p$ . Compared to previous emission  
 inventories, these high-resolution gridded datasets of crop planting area and livestock population allow us to develop a high-  
 resolution crop- and livestock-specific NH<sub>3</sub> emission inventory.

删除了: S7

删除了: We created

删除了: .

## 2.2. Atmospheric chemical transport model

The GEOS-Chem atmospheric chemistry model ([www.geos-chem.org](http://www.geos-chem.org), last accessed: November 2024), initially described by Bey et al. (2001), serves as an open-source global 3-D atmospheric chemical transport model encompassing detailed ozone–NO<sub>x</sub>–VOC–aerosol–halogen chemistry. It can conduct offline simulations driven by assimilated meteorological data the Goddard Earth Observing System (GEOS) of the NASA Global Modeling and Assimilation Office (GMAO) (<http://acmg.seas.harvard.edu/geos/>, last accessed: November 2024). For this study, we utilized the Modern-Era Retrospective Analysis for Research and Applications, version 2 (MERRA-2) meteorological data (Gelaro et al., 2017) for 1979–present at a horizontal resolution of  $0.5^\circ \times 0.625^\circ$  and 72 vertical levels. Our investigation employed the GEOS-Chem High Performance model (GCHP) version 13.2.1. The flexibility and scalability of high-resolution simulations in the GEOS-Chem Classic (GCC) model were limited, as it relies on shared-memory parallelization and a rectilinear longitude-latitude grid (Martin et al., 2022). GCHP, leveraging an identical GCC codebase, offers enhanced atmospheric chemical simulation capabilities, having evolved into a distributed-memory, modeling and analysis prediction layer (MAPL)-based rendition of GCC. By integrating a more efficient cubed-sphere grid and the finite-volume cubed-sphere dynamical core (FV3) advection, GCHP version 13 can operate on a stretched cubed-sphere grid to amplify grid resolution in a customized region with smooth, gradual resolution transitions (Eastham et al., 2018).

To improve simulation performance in China, Tsinghua University has developed localized emission inventories (MEIC), including SO<sub>2</sub>, NO<sub>x</sub>, NH<sub>3</sub>, carbon monoxide (CO), non-methane volatile organic compound (NMVOC), black carbon (BC), and organic carbon (OC) for China at  $0.25^\circ \times 0.25^\circ$  spatial resolution (<http://meicmodel.org/>, last accessed: October 2023) (Li et al., 2017). MEIC inventory has been widely used in Chinese studies, and serves as the common input of GCHP for the China domain. However, the NH<sub>3</sub> emission inventory in MEIC lacks crop- and livestock-specific emissions, and the coarser resolution constrains our understanding of the impact of NH<sub>3</sub> on PM<sub>2.5</sub>. Therefore, in this study we developed high-resolution crop- and livestock-specific NH<sub>3</sub> emission inventory as described above, which replaced the original MEIC NH<sub>3</sub> inventory in our simulations. Finally, we conducted PM<sub>2.5</sub> simulations for the year 2017 at  $0.5^\circ \times 0.5^\circ$  resolution (stretch factor = 4.0, target latitude =  $33^\circ\text{N}$ , and target longitude =  $109.4^\circ\text{E}$ ). Finally, the population-weighted PM<sub>2.5</sub> (PM<sub>2.5,p</sub>,  $\mu\text{g m}^{-3}$ ) is utilized to evaluate the air quality benefits of NH<sub>3</sub> reductions, which can be calculated as:

$$\text{PM}_{2.5,p} = \frac{\sum_i^n (\text{Pop}_i \times \text{PM}_{2.5,i})}{\sum_i^n \text{Pop}_i} \quad (6)$$

where  $\text{Pop}_i$  and  $\text{PM}_{2.5,i}$  ( $\mu\text{g m}^{-3}$ ) are the population and PM<sub>2.5</sub> concentration for grid cell  $i$ , respectively.

The accuracy of our newly developed agricultural NH<sub>3</sub> emission inventory was evaluated against available surface concentrations and other existing inventories. The instrument of Infrared Atmospheric Sounding Interferometer (IASI) detects NH<sub>3</sub> by measuring the absorption of infrared radiation emitted from the Earth's surface and atmosphere, and the measured

NH<sub>3</sub> is provided in the form of total column density. Liu et al. (2022) used IASI NH<sub>3</sub> columns and NH<sub>3</sub> vertical profiles simulated by GEOS-Chem to derive surface NH<sub>3</sub> concentrations, showing high consistency with ground observations in China. Specifically, they first simulated the NH<sub>3</sub> concentrations in 72 vertical layers via GEOS-Chem. The cumulative concentrations from these layers were aggregated to represent the column concentration. Next, they calculated the proportion of surface concentration to the total column concentration based on the simulated NH<sub>3</sub> vertical profiles. Finally, this ratio was applied to derive the surface NH<sub>3</sub> concentration from IASI NH<sub>3</sub> columns. The surface NH<sub>3</sub> concentrations simulated using our inventory and MEIC NH<sub>3</sub> were compared and further validated using their IASI-derived data. Moreover, PM<sub>2.5</sub> concentrations served as an additional metric to evaluate the performance of our inventory against MEIC NH<sub>3</sub> inventory. The PM<sub>2.5</sub> data in 2017 were collected from the Chinese Ministry of Ecology and Environment (MEE) (<https://quotsoft.net/air/>, last accessed: October 2023).

### 2.3. Nitrogen use efficiency

NUE is defined in this study as the ratio of the N input that can be transferred to the N contained in the product, calculated as the total N content in the product divided by the total N input (Gu et al., 2017). The N input of crop systems includes N content in fertilizer application, manure used as fertilizer, atmospheric deposition, irrigation, and biological fixation. The output N of crop systems is the N content in the harvested crops. For livestock systems, the N input mainly refers to feed N (e.g., forage, grain, and straw feed), and output N is N contained in animal products (e.g., meat and leather). NUE for crop and livestock systems can be expressed as:

$$NUE_{\text{crop}} = \frac{N_{\text{harvested}}}{N_{\text{input}}} \quad (7)$$

$$NUE_{\text{livestock}} = \frac{N_{\text{animal products}}}{N_{\text{input}}} \quad (8)$$

The Coupled Human And Natural Systems (CHANS) Nitrogen Cycling Model, a mass balance model for N budget, was employed to evaluate NUE in different crop and livestock subsystems. This model allows us to assess the N budget based on mass flows in seven compartments: industry, cropland, livestock, human, atmosphere, hydrosphere, and others (Gu et al., 2015). It incorporates socioeconomic data, land use patterns, and human behaviors to capture the human-driven processes affecting N inputs, such as fertilizer use and livestock production. The CHANS model was downloaded from <https://person.zju.edu.cn/bjgu> (last accessed: March 2024), and the required input datasets were updated in 2017 by the National Bureau of Statistics of China. Due to data limitations, we evaluated N budgets in six cropland subsystems (rice, wheat, maize, orchard, vegetables, and other crops) and four livestock subsystems (cattle, sheep & goat, pork, and poultry) at a provincial scale.



#### 2.4. Scenario analysis

With the help of the CHANS model, four abatement pathways were designed to identify the NH<sub>3</sub> mitigation potential. These scenarios are expected to improve NUE and reduce nitrogen losses in agricultural systems. The performance of abatement scenarios was examined by their mitigation efficiency, represented by the ratio of NH<sub>3</sub> emission reduction to baseline NH<sub>3</sub> emission. The available measures to achieve these scenarios with mitigation efficiency in China are shown in Table S9 and S10. The abatement scenarios include:

- (i) NUE-C scenario: improving the NUE of cropland systems. The excessive use of anthropogenic N application in croplands has been proven to be a problem in China. Several measures can be taken to enhance NUE to address this issue, such as adopting machine injection, optimal fertilizer application rate, and 4R principles (the right time, right amount, right form, and right method). According to farm surveys in China, the top 20 % of farmers in terms of crop NUE perform well in the nutrient management of farmlands. Specifically, the NUE of rice, wheat, maize, fruits, vegetables, and other crops are 0.66, 0.66, 0.66, 0.38, 0.70, and 0.68, respectively, for such top 20 % of farmers in China (Zhang, 2021). Here, we set the crop NUE of such top 20 % of farmers in China as the targeted NUE under this scenario.
- (ii) OUR scenario: improving organic fertilizer use ratio for crops. Livestock N excretion increases inevitably with increasing livestock population. Poor excretion N recycling rate attributable to low organic fertilizer use ratio results in massive NH<sub>3</sub> escape. In addition to substituting synthetic fertilizer, optimal organic fertilizer use could enhance the quality of soil and crop products. Studies in Europe and China all suggested that 50 % would be the optimal organic fertilizer use ratio (Sutton et al., 2022; Zhang, 2021). Therefore, under this scenario, the organic fertilizer use ratio is increased to 50 %.
- (iii) NUE-L scenario: improving the NUE of livestock systems. The key to improving the NUE of livestock systems is to increase the nutrient retention rate. Effective measures can be conducted during the feeding stage, including low crude protein feeding and dietary additives (Zhang et al., 2020), which can help reduce livestock N excretion. Other efforts to advance herd management are also needed to reduce livestock mortality. Under this scenario, we assumed that the NUE of livestock in China could be improved to the European level by adopting advanced farming practices. The livestock-specific targets are boosting NUE of cattle, sheep & goat, pork, and poultry to 0.26, 0.26, 0.35, and 0.55, respectively (Zhao et al., 2016; Groenestein et al., 2019).
- (iv) COMB scenario: combined measures. NH<sub>3</sub> emission reduction should not be limited to individual systems since collaborative efforts can lead to more impactful outcomes. Under the combined scenario, targets in NUE-C, OUR, and NUE-L are all expected to be realized.

We followed the bottom-up estimation methods in section 2.1 to generate new agricultural NH<sub>3</sub> emission estimates for these abatement scenarios accordingly. Specifically, the improvements of crop NUE and organic fertilizer use ratio result in lower synthetic fertilizer use, consequently mitigating the fertilizer-related NH<sub>3</sub> emissions. Meanwhile, the improvement of livestock NUE reduces the EFs of livestock, hereby contributing to a decrease in livestock-related NH<sub>3</sub> emissions. These revised agricultural NH<sub>3</sub> emission estimates were then used to drive GCHP to simulate corresponding changes in PM<sub>2.5</sub> levels from the non-abatement control scenario.

### 3. Results and discussion

#### 3.1. NH<sub>3</sub> emission of China in 2017

##### 3.1.1. Specific sources of agricultural NH<sub>3</sub> emissions

In 2017, fertilizer NH<sub>3</sub> emissions in China are estimated to be 5.17 Tg NH<sub>3</sub>, while NH<sub>3</sub> volatilization from livestock manure is 6.01 Tg NH<sub>3</sub>. Considering the 2.01 Tg NH<sub>3</sub> of non-agricultural emissions provided by MEIC inventory, the total NH<sub>3</sub> emissions amount to 13.2 Tg NH<sub>3</sub>. Agriculture is the primary source of NH<sub>3</sub> emissions, accounting for 84.8 % of total emissions. Fig. 1 presents the specific sources of agricultural NH<sub>3</sub> emissions. Among the fertilizer-related NH<sub>3</sub> emissions, maize cultivation makes the largest contribution (23.1 %), followed by rice (18.7 %) and wheat (16.5 %). Notable NH<sub>3</sub> emissions can also be found in vegetables (15.1 %) and fruits (9.4 %). Regarding NH<sub>3</sub> emissions from livestock manure, the largest contributor is cattle, accounting for 32 %, followed by pork (26.6 %), sheep & goat (20.4 %), and poultry (17.6 %). Moreover, we compared our agricultural NH<sub>3</sub> emissions with precious estimates (Table 1). Discrepancies in estimating NH<sub>3</sub> emissions stemming from livestock waste across various studies are generally minor, mostly concentrated in the range of 5–6 Tg NH<sub>3</sub> yr<sup>-1</sup>. However, there are notable discrepancies in fertilizer-related NH<sub>3</sub> emissions, varying from 2.8–7 Tg NH<sub>3</sub> yr<sup>-1</sup>. These uncertainties primarily arise from differences in the use of EFs, such as EDGAR and CEDS not using localized EFs in China, whereas we employed localized EFs in China.

295 **Figure 1.** Different NH<sub>3</sub> emission sources associated with fertilizer application (a) and livestock manure (b).

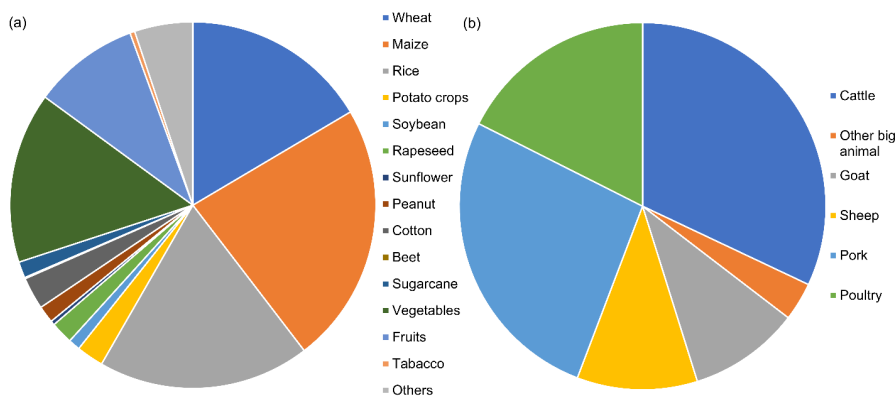


**Table 1.** Comparison of agricultural NH<sub>3</sub> emissions with precious estimates in China (Tg NH<sub>3</sub> yr<sup>-1</sup>)

Data source	Year	Fertilizer application	Livestock waste
Zhang et al. (2018)	2008	5.05	5.31
Li et al. (2021)	2016	4.67	5.42
Fu et al. (2020)	2016	3.88	5.18
Zhang et al. (2017)	2015	5.8	6.6
Wang et al. (2021)	2017	4.3	
Xu et al. (2015)	2010	4.48	5.08
Kang et al. (2016)	2012	2.81	5.03
Yang et al. (2023)	2017	6.55	7.3
EDGAR	2017	8.49	
CEDS	2017	9.61	
MEIC	2017	9.61	
REAS <sup>a</sup>	2015	8.4	2.8
This study	2017	5.17	6.01

<sup>a</sup> Manure-related NH<sub>3</sub> emissions in REAS do not include the manure applied as fertilizer to croplands, which contributes to fertilizer-related NH<sub>3</sub> emissions instead.

300 Cereal crops, such as wheat, maize, and rice, are extensively cultivated in China, encompassing 58.9% of the total planted

area (NBSC, 2023). With a high N fertilizer application rate ( $170\text{--}223\text{ kg N ha}^{-1}$ ), the cultivation of cereal crops results in 3.01 Tg  $\text{NH}_3$  emissions in 2017. Additionally, vegetable and orchard areas, accounting for 20 % of the total planted area, receive 30 % of synthetic fertilizers applied in China (Wang et al., 2022). Nitrogen management should be prioritized for the five crop types mentioned above, which accounted for over 80 % of fertilizer-related  $\text{NH}_3$  emissions. Remarkably, the overuse of synthetic fertilizers in vegetables and fruits is more severe than in cereal crops but has not received widespread attention (Wang et al., 2022). A 2–5-fold higher N fertilizer application rate in orchards and vegetables compared to cereal crops has been observed in China (Yu et al., 2022). Therefore, more effort is required to improve fertilization management in vegetables and orchards. Cattle holds a dominant position in  $\text{NH}_3$  emissions from livestock waste, both in China and globally, due to their large population and high N excretion. However, unlike other countries, pork contributes significantly to  $\text{NH}_3$  emissions in China. As the largest pork producer and consumer globally, China bears a high environmental cost of pork production (Bai et al., 2019). The contribution of pork to ambient  $\text{NH}_3$  concentration is well-documented, with national average  $\text{NH}_3$  concentrations recorded to be 3 % lower during the African swine fever period (July to December 2018) than historical levels (Liu et al., 2021). Meat consumption is projected to continue rising with population and income growth, further exacerbating such environmental burdens (Whitnall and Pitts, 2019). Therefore, it is crucial to improve livestock manure management to mitigate  $\text{NH}_3$  emissions.

### 3.1.2. Spatiotemporal distribution of $\text{NH}_3$ emissions

Consistent with ground-based observations (Pan et al., 2018),  $\text{NH}_3$  emissions are highest in summer, followed by spring, with weaker emissions in autumn and winter (Fig. 2). Rice and maize are responsible for high fertilizer-related  $\text{NH}_3$  emissions in summer. Meanwhile, winter wheat is the primary source of fertilizer-related  $\text{NH}_3$  emissions in autumn. On the other hand,  $\text{NH}_3$  emissions associated with livestock waste exhibit weak monthly variations, which are only induced by meteorological variations (Fig. 2b). Due to high temperatures, the strongest  $\text{NH}_3$  emissions from livestock waste happen in summer, a pattern that is also evident in satellite observations of the  $\text{NH}_3$  emissions from livestock farms (Liu et al., 2022).

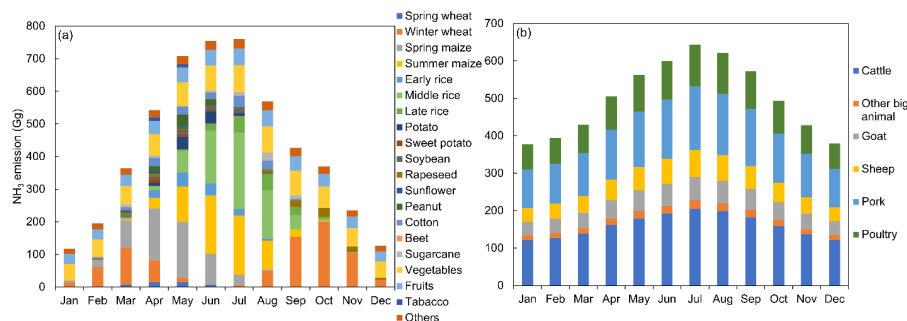


**Figure 2.** Monthly NH<sub>3</sub> emissions of specific crops (a) and livestock types (b).

Fig. 3 provides detailed NH<sub>3</sub> emissions spatial patterns with a high resolution at 1 km. NH<sub>3</sub> emissions are highly spatially heterogeneous, with the highest emissions in Southwest China and North China Plain, where agricultural activities are intensive. The provinces with the highest NH<sub>3</sub> emission intensities are Henan (67.2 kg NH<sub>3</sub> ha<sup>-1</sup>), Shandong (63.6 kg NH<sub>3</sub> ha<sup>-1</sup>), and Jiangsu (58.6 kg NH<sub>3</sub> ha<sup>-1</sup>), with emissions much higher than the national average (13.7 kg NH<sub>3</sub> ha<sup>-1</sup>). The NH<sub>3</sub> emission intensities attributable to fertilizer are also high in these provinces, with Jiangsu having the highest intensity (37.6 kg NH<sub>3</sub> ha<sup>-1</sup>) followed by Henan (36.2 kg NH<sub>3</sub> ha<sup>-1</sup>) and Shandong (25.2 kg NH<sub>3</sub> ha<sup>-1</sup>) (Fig. 3b). The distributions of agricultural sub-regions and provinces can be found in Fig. 3d and Table S11. The Huang-Huai-Hai (HHH) region is a major food production base in China, where approximately 30 % of total agricultural products are produced (Li et al., 2021). Henan province in this region has the largest fertilizer-related NH<sub>3</sub> emissions (604 Gg). In comparison, Heilongjiang province, another major grain-producing province with a similar yield to Henan, has only 190 Gg of fertilizer-related NH<sub>3</sub> loss. This could be explained by the better nutrient management of croplands, which will be discussed in section 3.2, and the lower temperature in Heilongjiang. Notably, Sichuan Basin and Guanzhong Plain also experience substantial NH<sub>3</sub> volatilization. Sichuan and Shaanxi, despite having lower agricultural products than Heilongjiang (NBSC, 2023), have greater NH<sub>3</sub> emissions (Sichuan: 217 Gg, Shaanxi: 229 Gg). In addition, Hubei and Hunan exhibit high emissions due to the extensive rice cultivation and hot weather. The NH<sub>3</sub> hotspots in Guangdong are mostly due to tropical vegetables and fruits.

As for NH<sub>3</sub> emissions from livestock waste, Shandong (28.1 kg NH<sub>3</sub> ha<sup>-1</sup>) and Henan (22.1 kg NH<sub>3</sub> ha<sup>-1</sup>) have high emission intensities (Fig. 3c) due to the presence of numerous intensive livestock farms. Unlike previous spatial patterns found for livestock waste-related NH<sub>3</sub> emissions, our results reveal large amounts of NH<sub>3</sub> emitted in many point sources. Emission hotspots exist in HHH, Sichuan basin, Hubei, and Hunan provinces. The highest emissions are found in Sichuan (477 Gg), primarily due to cattle (163 Gg) and pork (157 Gg). Similarly, in Hunan, the large magnitude of pork production leads to 142 Gg of NH<sub>3</sub> emissions. Notable NH<sub>3</sub> emissions also occur in Shandong (442 Gg), dominated by pork (117 Gg) and poultry (147

删除了: S8

355

Gg). In Northwest China, the largest contributors are cattle and sheep & goat. The different major contributors of livestock waste-related NH<sub>3</sub> emissions highlight the significant regional variations in dietary habits across China, necessitating different approaches for NH<sub>3</sub> control actions. We acknowledge the disparities in estimating livestock waste-related NH<sub>3</sub> emissions. For example, our poultry NH<sub>3</sub> estimates differ from those reported by Xu et al. (2015) and Gao et al. (2013). Likely reflecting uncertainties in raising days and livestock numbers.

设置了格式: 字体: 10 磅, 非加粗

设置了格式: 字体: 10 磅, 非加粗

360

**Figure 3.** Provincial total NH<sub>3</sub> emissions (a), and the spatial distribution of NH<sub>3</sub> emissions from fertilizer application (b), livestock waste (c); Agricultural sub-regions and provinces distribution in China (d). Agricultural sub-regions include Huang-Huai-Hai region (HHH), Middle and Lower Yangtze River region (MLYR), Northwest region (NW), Northeast region (NE), Southwest region (SW), and Southern China region (SC).

365

The seasonal cycle of NH<sub>3</sub> emissions from fertilizer is closely linked to crop cultivation and fertilizer application calendars (Li et al., 2021). The main growth stages for maize and rice are between May and July, during which a large amount of fertilizer is applied. Promoted by the warm weather, the highest NH<sub>3</sub> emissions occur during these three months (Fig. 2a). The numbers of animals kept in different months in China are unavailable, which may obscure the monthly differences in livestock waste-related NH<sub>3</sub> emissions. Even though the dynamics between livestock stock numbers and slaughter numbers are unknown, the total annual numbers are recorded so that the estimates of total livestock waste-related emissions are mostly reliable. As for spatial distribution, high fertilizer-related NH<sub>3</sub> emissions reflect high N fertilizer application rate, extensive planted area, and cropland intensity (ratio of total sown area of crops to cropland area). For example, in Jiangsu (the province with the highest fertilizer-related emissions), the N fertilizer application rates of rice, wheat, and maize are 1.91, 1.54, and 2.04 times higher

370

than the national average, respectively (NBSC, 2023). Moreover, the cropland intensity of Jiangsu in 2017 was 1.65, exceeding the national average (1.23). Compared to fertilizer-related  $\text{NH}_3$  emissions, Southwest and Central China exhibits high livestock waste-related  $\text{NH}_3$  emissions, especially in the Sichuan province. The meat consumption per capita in Sichuan is the highest in China, with a value of  $39.3 \text{ kg yr}^{-1}$  in 2015 (Song et al., 2019). Subsequently, the strong demand has expanded local pork production, threatening local air and water quality.

### 3.1.3. Evaluation of $\text{NH}_3$ emission inventory

Fig. 4 shows the annual mean ground-level atmospheric concentrations of  $\text{NH}_3$  and  $\text{PM}_{2.5}$  simulated by GCHP based on our new inventory and the MEIC inventory in 2017. The IASI-derived  $\text{NH}_3$  concentrations and observed  $\text{PM}_{2.5}$  concentrations were utilized to assess model performance. The surface  $\text{NH}_3$  concentrations exhibit similar spatial patterns to  $\text{NH}_3$  emissions, and the simulated  $\text{NH}_3$  concentrations from both inventories align well with satellite-derived observations. The simulated  $\text{NH}_3$  concentration driven by our inventory shows better spatial correlation with satellite observations ( $R = 0.90$ ), with a lower root mean square error (RMSE) of  $1.93 \mu\text{g N m}^{-3}$ . In comparison, the performance of MEIC is relatively lower ( $R = 0.84$ ), with an RMSE of  $2.59 \mu\text{g N m}^{-3}$ . High-concentration regions, identified at the junctions of Hebei, Shandong, and Henan provinces through satellite monitoring (Fig. 4a), are successfully reproduced by our inventory (Fig. 4c). In contrast, MEIC only generates the high-concentration cluster only in central Henan (Fig. 4e). Furthermore, compared to the average IASI-derived  $\text{NH}_3$  of HHH ( $14.5 \mu\text{g N m}^{-3}$ ), the modeled  $\text{NH}_3$  concentration is relatively lower, i.e.,  $10.5 \mu\text{g N m}^{-3}$  by our inventory and  $7.73 \mu\text{g N m}^{-3}$  by MEIC. It is noteworthy that the total  $\text{NH}_3$  emissions for China in 2017 were estimated to be  $10.3 \text{ Tg NH}_3$  by MEIC, which may be an underestimation. Additionally, we examined the seasonality of  $\text{NH}_3$  concentrations for sub-regions in Table S6 and conducted seasonal comparison between simulation and observations in Table S7. The temporal correlation between IASI-derived  $\text{NH}_3$  and  $\text{NH}_3$  modeled by our inventory is better than that for MEIC. Our inventory demonstrates superior accuracy in modeling surface  $\text{NH}_3$  concentrations compared to MEIC in all seasons, particularly during summer. Regarding  $\text{PM}_{2.5}$ , simulations with our inventory exhibit a stronger spatial correlation with observations than with MEIC, although concentrations are slightly overestimated. In HHH, a hotspot of  $\text{NH}_3$  emissions, our inventory excels in capturing monthly variations in surface  $\text{NH}_3$  concentrations, displaying a temporal correlation of 0.57 with IASI-derived  $\text{NH}_3$  concentrations that surpasses the correlation of 0.15 for MEIC.

设置了格式：下标

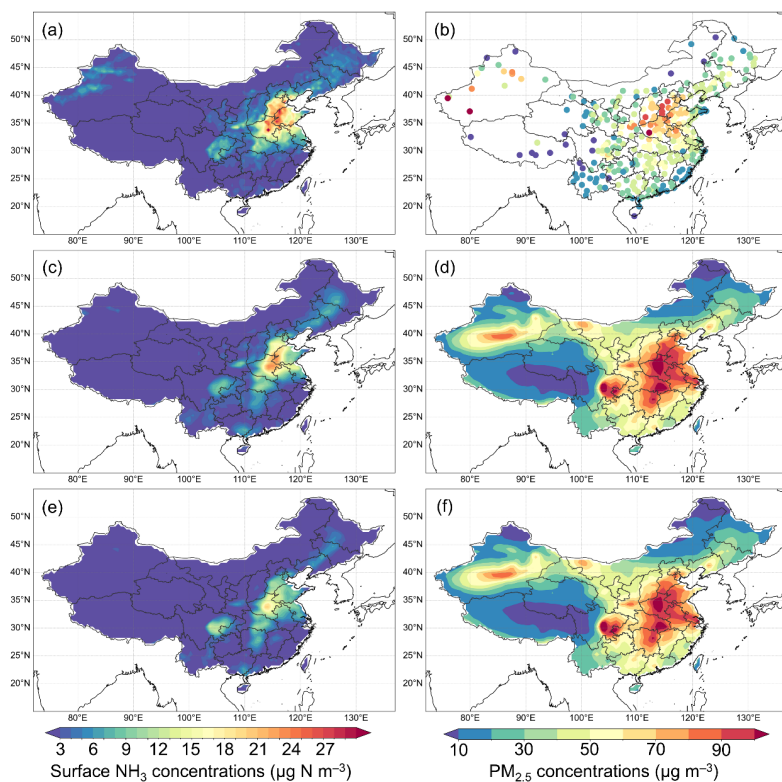


**Figure 4.** IASI-derived surface  $\text{NH}_3$  concentrations (a) and observed  $\text{PM}_{2.5}$  concentrations (b). The annual mean surface  $\text{NH}_3$  concentration in 2017 simulated by our inventory (c) and MEIC (e). The annual mean ground-level  $\text{PM}_{2.5}$  concentration in 2017 simulated by our inventory (d) and MEIC (f).

The  $\text{PM}_{2.5}$  simulation errors in GCHP driven by our inventory and MEIC are similar across China. The spatial correlation between simulations and field measurements ( $n = 363$ ) is slightly improved with our inventory ( $R = 0.66$ ) over MEIC ( $R = 0.64$ ). The improvement is observed in HHH, where the spatial correlation has increased from 0.46 (MEIC) to 0.53 (our inventory). In terms of annual mean bias, the RMSE of our inventory is  $26.6 \mu\text{g m}^{-3}$ , slightly higher than the  $26.2 \mu\text{g m}^{-3}$  of MEIC. However, it should be noted that GCHP tends to overestimate  $\text{PM}_{2.5}$  concentrations, particularly in the Sichuan Basin, Hubei, and Hunan provinces, which aligns with previous research findings (Xie and Liao, 2022; Zhai et al., 2021). The  $\text{NH}_3$  emissions in this study are higher than in MEIC, while the emissions of all other air pollutant emissions are from the MEIC. As a result, the simulated  $\text{PM}_{2.5}$  concentrations driven by our inventory (annual mean =  $37.2 \mu\text{g m}^{-3}$ ) are slightly higher than that of the MEIC (annual mean =  $36.3 \mu\text{g m}^{-3}$ ).



The overestimation of PM<sub>2.5</sub> concentrations in GEOS-Chem is a well-known issue in China. Several studies, including Xie & Liao (2022) and Zhai et al., (2021), reported that the model consistently overestimates PM<sub>2.5</sub> levels. Specifically, the modeled PM<sub>2.5</sub> concentrations in 2017 were 15.1 % higher than the observed values, and summer PM<sub>2.5</sub> concentrations in North China were overestimated by up to 33 % in 2016. The overestimation is primarily attributed to the overestimation of nitrate in the model, especially during nighttime periods (Zhai et al., 2021; Miao et al., 2020; Chen et al., 2019). The simulation performance for ammonium in GEOS-Chem is found to be superior to that of nitrate, with only a 6 % deviation from measured values (Miao et al., 2020). The overestimation of nitrate may arise from uncertainties in emission data, meteorological conditions, and modeled chemical mechanisms. Improving the representation of chemical processes is crucial for addressing this issue (Miao et al., 2020). A better understanding of the atmospheric reactive nitrogen budget, particularly the role of photolysis of particle-phase nitrate, is necessary. Furthermore, model investigation can benefit from simultaneous measurements of major reactive nitrogen species, which can provide critical datasets for refining and evaluating the performance of GEOS-Chem.

### 3.2. Nitrogen use efficiency of agricultural systems

Fig. 5 illustrates the NUE of crops in China at the provincial level in 2017. The NUE of cereal crops is around 0.5, higher than that of economic crops. Orchards, on the other hand, tend to have the lowest NUE, which is consistent with previous reports (Zhang, 2021). Notably, Heilongjiang demonstrates the highest NUE values across various crops, including rice (0.82), wheat (0.83), maize (0.77), fruits (0.71), and the whole crop system (0.70). This is also the reason why the NH<sub>3</sub> losses in Heilongjiang are low. To better understand the spatial patterns of NUE, we divided mainland China into six agricultural sub-regions (definitions and distribution can be found in Fig. 3d and Table S11). The NUE of these sub-regions is shown in Fig. S4. In terms of rice, NE demonstrates the highest NUE with a value of 0.71, followed by SW (0.57) and MLYR (0.51). Rice-producing regions such as Jiangxi, Hunan, Hubei, and Sichuan have NUE values higher than the national average. In contrast, Jiangsu and Anhui, also major rice-producing areas, have lower NUE values of 0.44 and 0.43, respectively. Regarding the NUE of wheat, NE leads with a value of 0.78, followed by HHH (0.56) and MLYR (0.51), while SC is only 0.22. Henan, Shandong, and Anhui, the top three wheat-growing provinces, exhibit commendable nitrogen utilization with NUE values of 0.59, 0.60, and 0.61, respectively. However, with extensive wheat planting, Jiangsu and Hebei show lower NUE values of 0.45 and 0.47, respectively. For the NUE of maize, NE and HHH perform well, with NUE values of 0.67 and 0.55, respectively. Shaanxi and Yunnan, provinces with over 1,000 thousand hectares of maize cultivation, exhibit notably low NUE values of 0.26 and 0.33.

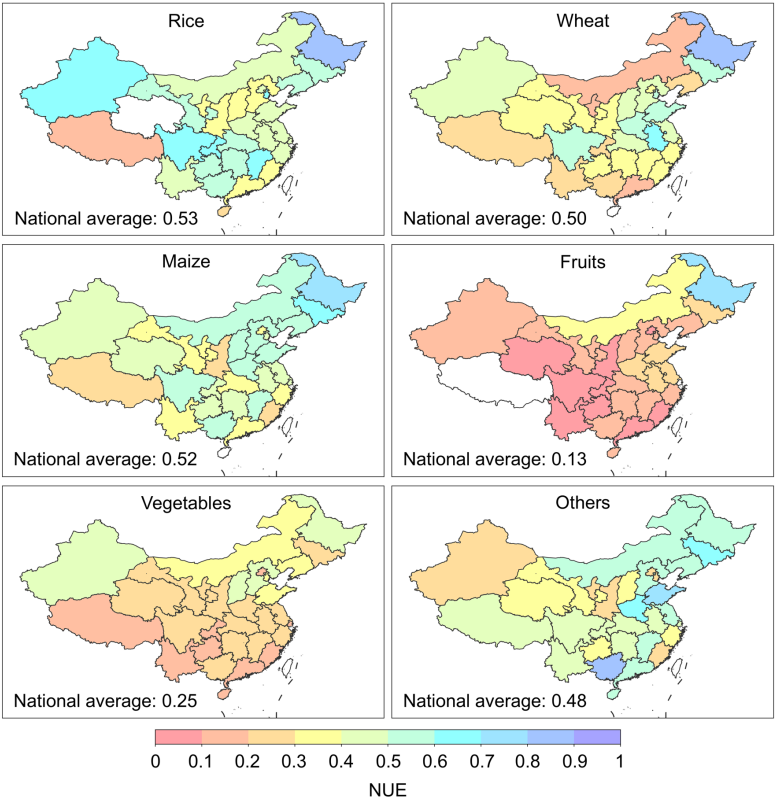
The N management in orchard areas is better in HHH (NUE: 0.21) and MLYR (NUE: 0.16). However, nine provinces,

删除了: ,

域代码已更改

删除了: S8

primarily in SW and SC, have the NUEs of fruits below 0.1, with the lowest NUE recorded in Qinghai at 0.03. For vegetables, NUE is higher in northern China than in the south. Higher values could be identified in NE (0.36), HHH (0.34), and NW (0.31). The poor N management in fruits and vegetables highlights the potential for NH<sub>3</sub> emissions. In addition to these major crops, we assessed the NUE of other crops (e.g., beans, potatoes, cotton, peanuts, rapeseed, sunflower, sugarcane, sugarbeet, tobacco, and tea). SC (0.69), HHH (0.65), and NE (0.56) display higher NUE than the national average. The estimated NUE patterns in the whole crop system, as depicted in Fig. S4a and Fig. S5a, show that the NUE follows a similar trend as previous results (Zhang, 2021), with the NE having the highest NUE, followed by the HHH, MLYR, SW, SC, and NW regions.



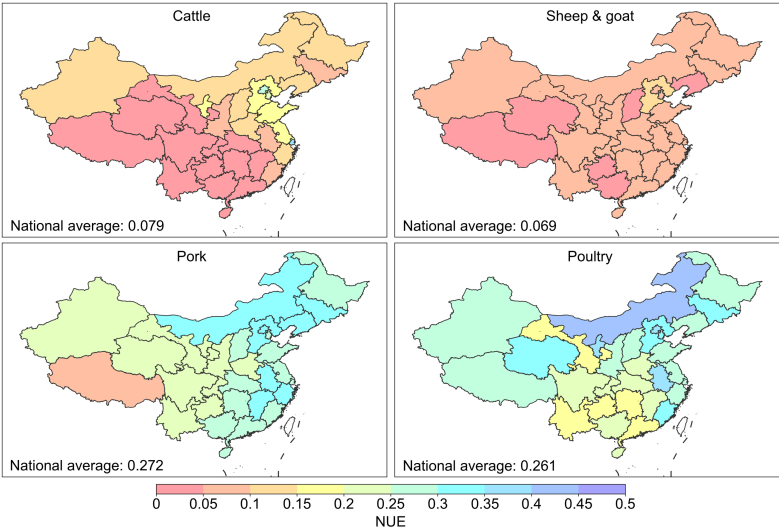
**Figure 5.** Nitrogen use efficiency of six crop types in China in 2017. The inserted values are the national average NUE for each crop type.

Fig. 6 presents the NUE of four livestock types in China. Similar to Bai et al., (2016), ruminants, including cattle, sheep and goat, have notably lower NUE compared to other animals. Specifically, the national average NUE of these ruminants is

删除了： ,

below 0.1. The type of livestock farm and its management level influence the NUE of whole livestock systems. In China, a west-to-east trend of increasing NUE of livestock systems is observed, as shown in Figure S6b. Similar NUE values and spatial patterns have been reported in another localized nitrogen budget model (NUFER model) (Jin et al., 2021; Bai et al., 2018). Based on this model, the NUE of ruminants and monogastric animals are ~0.05 and ~0.25, respectively. For cattle, the NUE is significantly higher in northern China (e.g., NE, HHH, and NW) than in the south (Fig. S5b). The highest NUE can be observed in Shanghai at 0.36, followed by Beijing (0.27) and Tianjin (0.23). These mega-cities have stricter environmental regulations and more willing to improve the management of livestock farms. In the case of sheep and goat, NUE for all provinces remains at a low level, ranging from 0.03 to 0.1, indicating poor N management level. The national average NUE of pork is 0.272, below the European level of 0.35. Higher NUE is found in NE, MLYR, and HHH. SW, having approximately a quarter of pork farms in the nation, is leading the way in N losses. Regarding the NUE of poultry, northern China also performs better than the south. The highest NUE (0.4) is observed in Inner Mongolia, which may be attributable to lower temperatures, and better N management also occurs in the Beijing-Tianjin-Hebei region. However, the NUE values for all provinces in China are lower than the European level of 0.55.

删除了: in



**Figure 6.** Nitrogen use efficiency of four livestock types in China in 2017. The inserted values are the national average NUE for each livestock type.

Organic fertilizer is also an important N source for crops. Due to the lack of precise data on organic fertilizer application

480 rates for different crops, we estimated the quantity of organic fertilizer used in each province based on previous studies and available information (Fig. 7) (Gu et al., 2015; Zhang et al., 2023). In 2017, 8.43 Tg N of organic nitrogen fertilizer was applied to croplands, representing only 22.2% of the total anthropogenic N inputs including organic and chemical sources. Among these inputs, livestock manure contributes 4.27 Tg N, while human excretion accounts for 1.81 Tg N and 2.35 Tg N originates from the crop straw recycling to the croplands. The CHANS model estimates a substantial N content of 14 Tg N yr<sup>-1</sup> in livestock excretion, indicating a sizeable synthetic fertilizer substitution potential through manure. However, these manure resources are spatially mismatched with croplands, which may increase the environmental risks induced by manure. For example, livestock manure N exceeds crop harvest N in Tibet, Beijing, Yunnan, Qinghai, and Gansu provinces. Furthermore, we examined the organic fertilizer use ratio (Fig 7a). Organic fertilizer use was significantly higher in western China, such as 47.8 % of Gansu and 32.2 % of Ningxia, compared to eastern China, such as Jiangsu (13.6 %) and Guangdong (15.5 %).

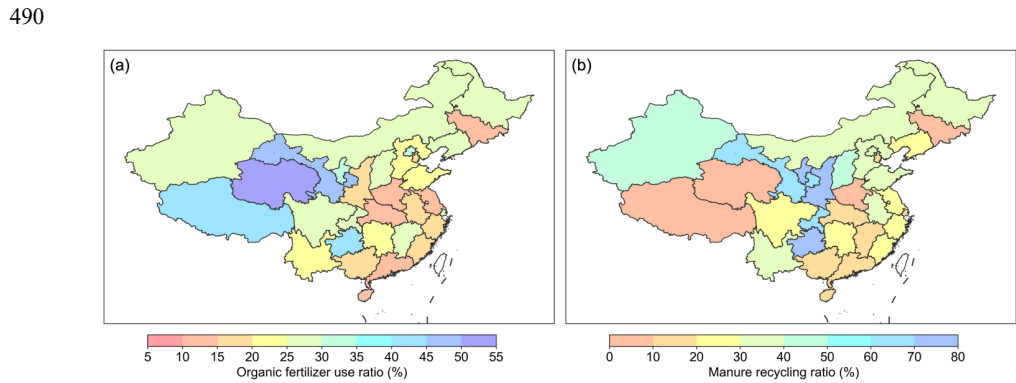


**Figure 7.** Organic fertilizer use ratio (a) and manure recycling ratio to cropland (b) derived from Zhang et al. (2023)

It is observed that NE performs better in managing the N of crop systems, especially in Heilongjiang, which benefits from favorable natural conditions and high agricultural mechanization. As a result, despite substantial agricultural production, Heilongjiang experiences minimal NH<sub>3</sub> losses. Recently, Liu et al. (2023) reported a noticeable improvement in the NUE of grain crops in China via regulated fertilizer use. Controlling fertilizer use to improve efficiency can also improve NUE. In addition, Due to the inability to accurately know the planting area of specific fruits and vegetables, this study only collectively evaluated nitrogen management levels for all fruits and vegetables. It is important to recognize that different fruit or vegetable types require varied N management practices, which can significantly affect NUE. For instance, in Shaanxi, where apple cultivation accounts for half of the orchard area, excessive fertilizer use is a serious issue in apple cultivation, resulting in a low NUE of 0.09 for the orchard (Zhang, 2021). Vegetables and fruits have lower NUE than grain crops, emphasizing the importance of improved N management practices for vegetable and fruit cultivation to reduce NH<sub>3</sub>.

Regarding ruminants, NUE is notably higher in the northern regions, including Ningxia, Hebei, and Inner Mongolia, where pastoral areas exhibit low nitrogen losses from grazing systems. Moreover, provinces with a prominent presence of industrial livestock farms, such as Beijing, Tianjin, and Shanghai, demonstrate NUE levels surpassing the national average. Considering the whole livestock systems, NUE is significantly higher in the economically developed and livestock-intensive eastern regions compared to the western regions. Industrial livestock systems tend to have better herd management with lower NH<sub>3</sub> emissions at the housing and storage stages of manure management. In the western regions, smallholders often adopt an integrated farming system, which enables timely manure recycling to croplands. In the eastern regions, more industrial livestock farms exacerbate the decoupling of crops and livestock, preventing manure from being used in the fields, which may increase NH<sub>3</sub> emissions from livestock waste. Therefore, despite the better management and production efficiency of industrial farms, if their large amounts of livestock manure are not treated promptly, NH<sub>3</sub> emissions from the entire agricultural systems would increase.

515

### 3.3. Scenario analysis

#### 3.3.1. Agricultural NH<sub>3</sub> emission reductions

Mitigation efficiencies were calculated based on the targets and baseline conditions of different scenarios, as shown in Fig. 8. The NUE-C scenario can reduce agricultural NH<sub>3</sub> emissions by 2.05 Tg NH<sub>3</sub> via a reduction in synthetic fertilizer use, with a mitigation efficiency of 18.3 %. In the major grain-producing regions, such as Heilongjiang, Jilin, Henan, and Inner Mongolia, the mitigation potential of improving NUE-C is limited (below 15 %). In contrast, Jiangsu, also a major grain-producing province, still has a significant potential for emission reduction, with a mitigation efficiency of 39.9 %. Shaanxi and Zhejiang also exhibit high abatement efficiency, surpassing 40 %. Another practical approach for reducing synthetic fertilizer use is increasing organic fertilizer use, which can help reduce 1.86 Tg NH<sub>3</sub> emissions. Compared to the NUE-C scenario, the OUR scenario is more effective in NE and HHH, while both options yield similar effects for Jiangsu, Shaanxi, and Guangdong. Improving the NUE of the livestock systems, similar to previous findings (Zhang et al., 2020), results in lower benefits compared to the NUE-C scenario. Only 1.25 Tg NH<sub>3</sub> emissions from livestock can be mitigated under the NUE-L scenario. Several provinces with large livestock populations, such as Henan, Hebei, and Hubei, show mitigation efficiencies of less than 10 %. Integrating the three pathways mentioned above could decrease 4.41 Tg NH<sub>3</sub> emissions, including 3.16 Tg fertilizer-related reductions and 1.25 Tg livestock waste-related reductions. Provinces in SC and MLYR exhibit mitigation efficiencies exceeding 40 %, with the highest observed efficiency of 52.9 % in Shaanxi.

530

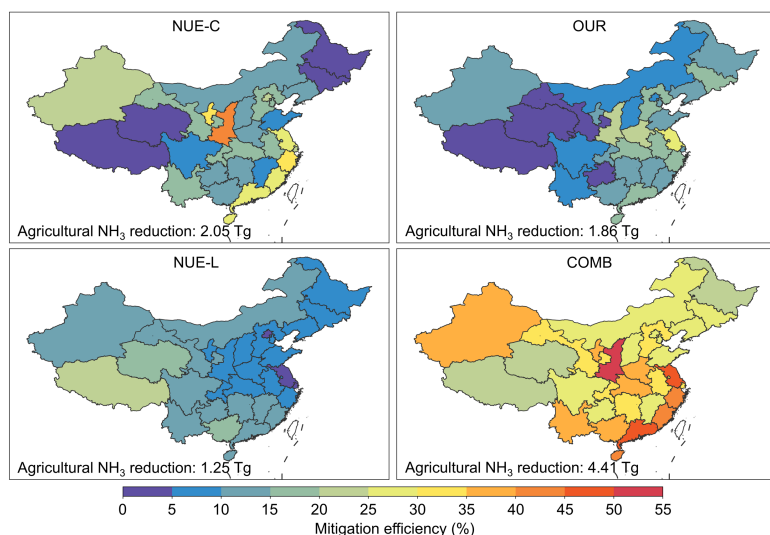


**Figure 8.** Mitigation efficiencies of NUE-C (a), OUR (b), NUE-L (c) and COMB (d) scenarios. Mitigation efficiency is the ratio of NH<sub>3</sub> emission reduction to baseline NH<sub>3</sub> emission.

We further examined the contribution of different crop and livestock types to emission reduction, which can help us identify areas where urgent efforts are needed (Fig. 9). Under the NUE-C scenario, synergic efforts with all crops are needed across China, with vegetables making the largest contribution at 25.6 %. Vegetables also hold a dominant position in HHH (31.8 %), MLYR (32.7 %), SW (33.9 %), and SC (37.9 %), reflecting the urgency to enhance N management of vegetables. Fruits also contribute significantly, particularly in SC (31.2 %). When comparing the NUE-C scenario to OUR+NUE-C, the importance of grain crops in grain-producing regions such as NE, HHH, and MLYR becomes more prominent with the improvement of organic fertilizer use (OUR). As for livestock, more efforts can be made in cattle, sheep and goat for SW and NW, while poultry and pork for SC, HHH and MLYR. Overall, across all provinces except Sichuan, the reduction of NH<sub>3</sub> emissions is primarily achieved through improvements in cropland systems (Table S9).

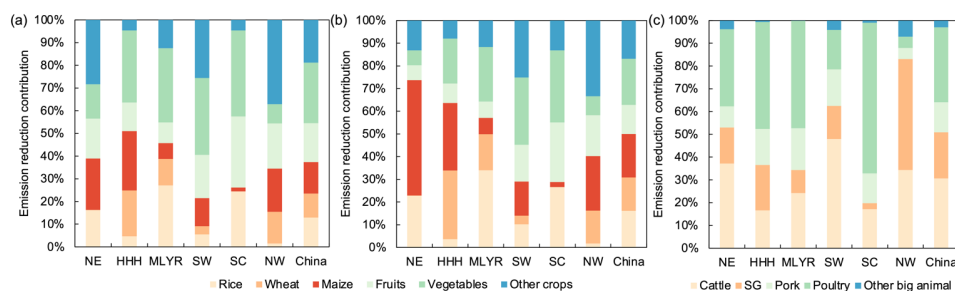


**Figure 9.** Contribution of different crop or livestock to emissions reductions under NUE-C (a), OUR+NUE-C (b) and NUE-L (c) scenarios

### 3.3.2. PM<sub>2.5</sub> reductions

Fig. 10 shows the benefits of different mitigation scenarios on PM<sub>2.5</sub> concentrations. The reductions are the most profound in central, eastern, and southern China. Under the NUE-C scenario, a 15.5 % reduction in NH<sub>3</sub> emissions leads to a 2.2 % decrease (0.83 μg m<sup>-3</sup>) in the annual average PM<sub>2.5</sub> concentration for China. Notably, significant improvements could be found in Zhejiang, with a 6.8 % reduction (4.1 μg m<sup>-3</sup>) in annual PM<sub>2.5</sub>. Shaanxi also demonstrates considerable reductions, with a 4.7 % decrease (2.8 μg m<sup>-3</sup>) in PM<sub>2.5</sub>. Under the OUR scenario, a 14.1 % reduction in NH<sub>3</sub> emissions results in a 1.9 % mitigation of the annual national average PM<sub>2.5</sub> (0.7 μg m<sup>-3</sup>). Hotspots of PM<sub>2.5</sub> reductions are observed in Henan (2.8 μg m<sup>-3</sup>), Hubei (2.7 μg m<sup>-3</sup>), and the junction of Anhui, Jiangsu, and Zhejiang (2.8–2.9 μg m<sup>-3</sup>). For NUE-L, the removal effects of PM<sub>2.5</sub> are relatively lower, with hotspots in the south. A reduction of 9.4 % in NH<sub>3</sub> emission has resulted in a 1.3 % decrease in annual PM<sub>2.5</sub> concentration (0.5 μg m<sup>-3</sup>) over China. Notable PM<sub>2.5</sub> reductions are found in Sichuan, Hunan, Guangdong, and Guangxi. For example, a 10.7 % NH<sub>3</sub> reduction leads to a 2.4 % PM<sub>2.5</sub> reduction (1.9 μg m<sup>-3</sup>) in Hunan. The national annual average PM<sub>2.5</sub> concentration experiences a decrease of up to 2.0 μg m<sup>-3</sup> via the integration of three measures. Regions such as Zhejiang, Hubei, and Hunan experience even more significant reductions, reaching nearly 7.0 μg m<sup>-3</sup>. The enhancement in air quality resulting from the decrease in NH<sub>3</sub> emissions per unit will escalate with the amplification of NH<sub>3</sub> emission reductions, indicating a nonlinear PM<sub>2.5</sub> response to NH<sub>3</sub> (Ye et al., 2019).

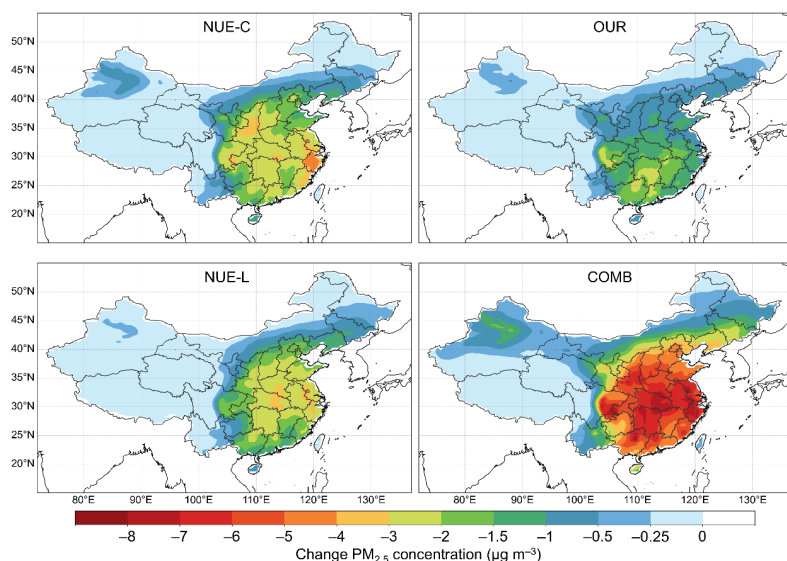


**Figure 10.** Changes of ground-level PM<sub>2.5</sub> concentration of different mitigation scenarios.

To better understand the public health benefits resulting from NH<sub>3</sub> abatements, we calculated population-weighted PM<sub>2.5</sub> (PM<sub>2.5,p</sub>) concentrations. It provides insights into the mitigation of human exposure in different regions during different seasons (Fig. 11). In 2017, the seasonal pattern of PM<sub>2.5,p</sub> followed the order: winter > autumn > spring > summer. The annual PM<sub>2.5,p</sub> declines by 1.8 µg m<sup>-3</sup>, 1.6 µg m<sup>-3</sup>, 1.3 µg m<sup>-3</sup>, and 4.1 µg m<sup>-3</sup> under NUE-C, OUR, NUE-L, and COMB scenarios, respectively. Compared to PM<sub>2.5</sub>, a larger decrease is observed in PM<sub>2.5,p</sub>, indicating greater health benefits could be obtained from NH<sub>3</sub> mitigation-related air quality improvements. The fertilizer-related control scenarios (NUE-C and OUR) demonstrate more significant benefits in summer and spring due to high fertilizer-related emissions during these seasons. Conversely, the livestock-related control scenarios (NUE-L) show greater benefits in winter. With high population density and NH<sub>3</sub> abatement efficiencies, MLYR and HHH exhibit higher health benefits. In the case of NUE-L, SW shows the highest outcomes, slightly surpassing SC and MLYR. On the other hand, NE consistently shows the lowest effects across all scenarios.



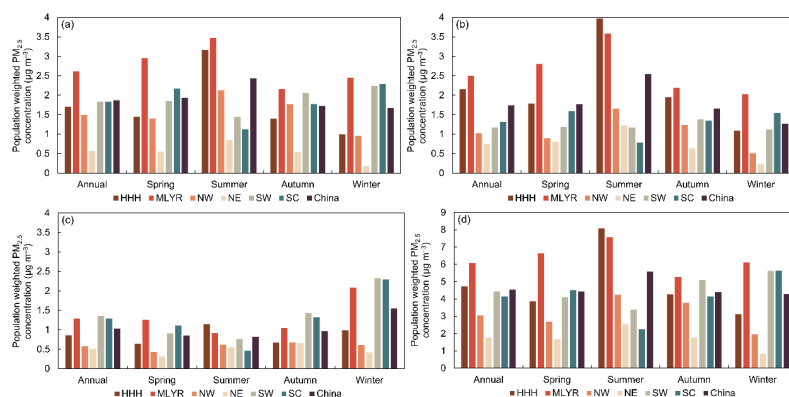


**Figure 11.** Seasonal population-weighted PM<sub>2.5</sub> concentration reductions under NUE-C (a), OUR (b), NUE-L (c), and COMB (d).

#### 4. Conclusions

This study aims to explore the relationships between agricultural NUE and air pollution, and further provides tailored recommendations (crop-, livestock-, and regional-specific) for NH<sub>3</sub> control in agriculture. To achieve this, we integrated a new NH<sub>3</sub> emission inventory, a nitrogen flow model, and air quality model for a comprehensive analysis. First, we estimated China's agricultural NH<sub>3</sub> emissions in 2017 based on the total use of synthetic fertilizers in croplands, livestock population, and their corresponding localized emission factors, accounting for the impacts of meteorological, soil, and management factors. Leveraging detailed spatial data on crop cultivation areas and livestock distribution, we utilized a bottom-up estimation method to develop crop- and livestock-specific NH<sub>3</sub> emission inventory at 1 km. Subsequently, the newly developed NH<sub>3</sub> emission inventory was incorporated into the GCHP model to simulate surface atmospheric NH<sub>3</sub> and PM<sub>2.5</sub> concentrations, with validation against observations. Finally, we employed the nitrogen flow model (CHANS) to explore the potential for agricultural NH<sub>3</sub> reduction under scenarios of increasing crop NUE, livestock NUE, and organic fertilizer usage. By establishing NH<sub>3</sub> emission inventories under such mitigation scenarios using the bottom-up estimation method, we then utilized the GCHP model to evaluate the air quality improvements resulting from NH<sub>3</sub> emission reductions.

Our findings reveal that improving NUE is crucial in reducing NH<sub>3</sub> emissions and mitigating air pollution. Furthermore, we provide more insights into which areas should be prioritized and what optimal outcomes can be realized for different regions. Specifically, efforts in cropland systems (i.e., improving NUE and organic fertilizer use) are more effective than in livestock systems (i.e., enhancing NUE). Spatial disparities also exist in the effects of mitigation options. For example, improving organic fertilizer use is projected to be an effective way to control NH<sub>3</sub> in grain-producing regions (e.g., HHH and

NE). On the other hand, improving crop NUE is profitable in southern coastal China and Shaanxi province. In terms of livestock systems, improving NUE can yield more significant benefits in the southern regions compared to the northern regions. Regarding specific species, although grain crops are responsible for substantial NH<sub>3</sub> losses from cropland systems, the NH<sub>3</sub> control of vegetables and fruits is much needed due to their severe overuse of synthetic fertilizers. It is noteworthy that the Chinese government launched the “Fertilizer Use Zero-Growth Action Plan by 2020” policy to control fertilizer use in 2015, which has dramatically reduced anthropogenic N inputs to croplands (Yu et al., 2022). This policy successfully reduces the N fertilizer use of grain crops, but limited progress has been observed in vegetables and fruits, appealing the need for further actions. Furthermore, though not specifically examined in this study, intervention measures on the food demand side can also be effective in reducing NH<sub>3</sub> emissions, such as reducing food loss and waste or adopting healthier, less meat-intensive diets to help reduce demand for agricultural products (Liu et al., 2021).

Since the initiation of China’s Air Clean Action Strategy in 2013, there have been significant reductions in SO<sub>2</sub> and NO<sub>x</sub> emissions, notably alleviating of PM<sub>2.5</sub> pollution. However, effective control measures for NH<sub>3</sub> emissions are lacking, potentially limiting further air quality improvements. It is noteworthy that the effectiveness of PM<sub>2.5</sub> control through NH<sub>3</sub> reduction will likely diminish as SO<sub>2</sub> and NO<sub>x</sub> levels decrease further (Liu et al., 2021c), because in NH<sub>3</sub>-rich environments, there may be a scarcity of adequate acidic gases to neutralize the NH<sub>3</sub>, thereby constraining ammonium formation. Nevertheless, the significance of NH<sub>3</sub> control via improving NUE remains. From a cost perspective, the expense of NH<sub>3</sub> abatement is only ~10% of that associated with NO<sub>x</sub> abatement (Gu et al., 2021). As China intensifies its efforts to reduce NO<sub>x</sub> emissions, the abatement costs are anticipated to rise. Furthermore, enhancing NUE not only curbs NH<sub>3</sub> emissions, but also lowers N<sub>2</sub>O emissions, nitrogen leaching to water, nitrogen deposition, and fertilizer expenses, thus offering climatic, ecological and socioeconomic co-benefits.

Our research has various limitations. Due to a lack of data, this study only considers the spatial distribution of grain crops. Although grain crops account for nearly 60 % of the cultivated area in China, the spatial distribution of other crops still influences the spatial pattern of NH<sub>3</sub> emissions. For livestock, although the year-end numbers are known, the monthly variations in the number of livestock are unavailable, which limits our understanding of the monthly changes of livestock-related NH<sub>3</sub> emissions. In addition, the lack of regional-specific EFs poses a challenge to accurately reproduce the spatial pattern of NH<sub>3</sub> emissions. About 20% of agricultural NH<sub>3</sub> emissions were evenly distributed using simplifying assumptions, which may have led to uncertainties in gridded allocation. Such uncertainties may induce biases in NH<sub>3</sub> and PM<sub>2.5</sub> mitigation assessment. We utilized the CHANS model to calculate NUE for crop and livestock systems; however, nitrogen budget models like this suffer uncertainties stemming from simplifications of the intricate nitrogen cycle and data deficiencies (Zhang et al., 2021a, b). The estimation uncertainty of nitrogen inputs was noted at ~10%, whereas nitrogen output uncertainty could soar

设置了格式: 字体: 10 磅

设置了格式: 字体: (中文) + 中文正文 (DengXian), 10 磅, 字体颜色: 文字 1, 英语(美国)

设置了格式: 字体: 10 磅

设置了格式: 字体: 10 磅

设置了格式: 字体: 10 磅

带格式的: 缩进: 左侧: 0 厘米, 首行缩进: 0.71 厘米, 段落间距段前: 0 磅, 段后: 0 磅, 行距: 1.5 倍行距

设置了格式: 字体: 10 磅

设置了格式: 字体: 10 磅

设置了格式: 字体: 10 磅

设置了格式: 字体: 10 磅

设置了格式: 字体: 10 磅

设置了格式: 字体: 10 磅

设置了格式: 字体: 10 磅

设置了格式: 字体: 10 磅

设置了格式: 字体: 10 磅, 非加粗

设置了格式: 字体: 10 磅

设置了格式: 字体: 10 磅

设置了格式: 字体: 10 磅

设置了格式: 字体: 10 磅, 非加粗

设置了格式: 字体: 10 磅

删除了: ↵

设置了格式: 下标

设置了格式: 下标

to ~30%, primarily due to challenges in accurately predicting nitrogen levels in individual agricultural products (Zhang et al., 2021b). As for the improved NUE scenarios, while a range of specific actionable strategies can be implemented (Table S9 and S10), it is crucial to acknowledge the challenges associated with executing these measures across different levels, considering the costs and anticipated outcomes. Moreover, our assumption of a simultaneous decrease in all nitrogen losses may not fully account for scenarios where certain measures prioritize NH<sub>3</sub> control over other forms of nitrogen loss mitigation. In future work, more data on agricultural practices needs to be collected to help us refine our analysis and policy recommendations.

Sustainable agriculture is farming in such a way as to satisfy human food needs, protect the environment, enhance the livelihoods of farmers, promote a more equitable society, and make the most efficient use of resources. It should be environmentally friendly, economically viable, and socially equitable, which is essential to help society achieve multiple Sustainable Development Goals (SDGs). More sustainable agriculture is directly linked to SDG2 “Zero Hunger” for providing enough food for humans, and should also help address SDG1 “No Poverty” for ensuring farmers’ livelihoods, SDG3 “Good Health and Well-being” for more nutritious food and less agricultural pollution, SDG13 “Climate Action” for reducing greenhouse gas emissions, and various others more indirectly. It should be noted that these SDGs need to be achieved in synchrony. For example, controlling synthetic fertilizer use at an optimal rate can simultaneously increase net profits, reduce NH<sub>3</sub> emissions, and ensure crop yields, thereby benefiting air quality. Our study provides a solid analysis and support for such a pathway. Despite the crucial role of the agricultural sector in emissions, emission reduction targets for this sector lag those set for the energy, industrial and transportation sectors. Currently, only the European Union (EU) has set NH<sub>3</sub> control targets, aiming to reduce NH<sub>3</sub> emissions by 19% in 2030 compared to 2005 levels (EU, 2016). In 2023, China announced new “Clean Air Actions”, which include NH<sub>3</sub> as a target for the first time ([https://www.gov.cn/zhengce/content/202312/content\\_6919000.htm](https://www.gov.cn/zhengce/content/202312/content_6919000.htm), last accessed: December 2024). However, specific targets have been assigned only to the Beijing-Tianjin-Hebei region, with a goal of a 5 % reduction by 2025 compared to 2020 levels. Our findings demonstrate that this target is attainable in the Beijing-Tianjin-Hebei region. We believe that our results can serve as an important reference for government to develop specific targets and plans to help better control agricultural NH<sub>3</sub> emissions toward clean air in the larger context of sustainable development.

**Data availability.** The NH<sub>3</sub> emission inventory are available on the open-access online repository:

<https://doi.org/10.6084/m9.figshare.28082276.v1>.

**Competing interests.** At least one of the (co-)authors is a member of the editorial board of Atmospheric Chemistry and Physics.

删除了: n summary, i

665

**Author contributions.** APKT conceived the study and supervised the writing of the paper. BL designed the study, conducted model simulations, analyzed the results, and wrote the draft. LL provided surface NH<sub>3</sub> datasets. DHYY, LTHN, JWZ, and TGY assisted in GEOS-Chem simulations and the interpretation of the results. All authors contributed to the discussion and improvement of the paper.

670

**Acknowledgements.** This work was supported by grants from the Hong Kong Research Grants Council (General Research Fund Grant no. 14307722) to APKT.

## Reference:

- 675 Abbatt, J. P. D., Benz, S., Czkzo, D. J., Kanji, Z., Lohmann, U., and Möhler, O.: Solid ammonium sulfate aerosols as ice nuclei: A pathway for cirrus cloud formation, *Science* (80-. ), 313, 1770–1773, <https://doi.org/10.1126/science.1129726>, 2006.
- Bai, Z., Ma, L., Jin, S., Ma, W., Velthof, G. L., Oenema, O., Liu, L., Chadwick, D., and Zhang, F.: Nitrogen, phosphorus, and potassium flows through the manure management chain in China, *Environ. Sci. Technol.*, 50, 13409–13418, <https://doi.org/10.1021/acs.est.6b03348>, 2016.
- 680 Bai, Z., Ma, W., Ma, L., Velthof, G. L., Wei, Z., Havlik, P., Oenema, O., Lee, M. R. F., and Zhang, F.: China's livestock transition: Driving forces, impacts, and consequences, *Sci. Adv.*, 4, <https://doi.org/10.1126/sciadv.aar8534>, 2018.
- Bai, Z., Jin, S., Wu, Y., Ermgassen, E. zu, Oenema, O., Chadwick, D., Lassaletta, L., Velthof, G., Zhao, J., and Ma, L.: China's pig relocation in balance, *Nat. Sustain.*, 2, 888–888, <https://doi.org/10.1038/s41893-019-0391-2>, 2019.
- 685 Battye, W., Aneja, V. P., and Roelle, P. A.: Evaluation and improvement of ammonia emissions inventories, *Atmos. Environ.*, 37, 3873–3883, [https://doi.org/10.1016/S1352-2310\(03\)00343-1](https://doi.org/10.1016/S1352-2310(03)00343-1), 2003.
- Behera, S. N., Sharma, M., Aneja, V. P., and Balasubramanian, R.: Ammonia in the atmosphere: A review on emission sources, atmospheric chemistry and deposition on terrestrial bodies, *Environ. Sci. Pollut. Res.*, 20, 8092–8131, <https://doi.org/10.1007/s11356-013-2051-9>, 2013.
- 690 Bey, I., Jacob, D. J., Yantosca, R. M., Logan, J. A., Field, B. D., Fiore, A. M., Li, Q., Liu, H. Y., Mickley, L. J., and Schultz, M. G.: Global modeling of tropospheric chemistry with assimilated meteorology: Model description and evaluation, *J. Geophys. Res. Atmos.*, 106, 23073–23095, <https://doi.org/10.1029/2001JD000807>, 2001.
- Bouwman, A. F., Boumans, L. J. M., and Batjes, N. H.: Estimation of global NH<sub>3</sub> volatilization loss from synthetic fertilizers and animal manure applied to arable lands and grasslands, *Global Biogeochem. Cycles*, 16, <https://doi.org/10.1029/2000gb001389>, 2002.
- 695 Chen, L., Gao, Y., Zhang, M., Fu, J. S., Zhu, J., Liao, H., Li, J., Huang, K., Ge, B., Wang, X., Lam, Y. F., Lin, C. Y., Itahashi, S., Nagashima, T., Kajino, M., Yamaji, K., Wang, Z., and Kurokawa, J. I.: MICS-Asia III: multi-model comparison and evaluation of aerosol over East Asia, *Atmos. Chem. Phys.*, 19, 11911–11937, <https://doi.org/10.5194/acp-19-11911-2019>, 2019.
- 700 Cheng, M., Quan, J., Yin, J., Liu, X., Yuan, Z., and Ma, L.: High-resolution maps of intensive and extensive livestock production in China, *Resour. Environ. Sustain.*, 12, 100104, <https://doi.org/10.1016/j.resenv.2022.100104>, 2023.
- Crippa, M., Solazzo, E., Huang, G., Guizzardi, D., Koffi, E., Muntean, M., Schieberle, C., Friedrich, R., and Janssens-Maenhout, G.: High resolution temporal profiles in the Emissions Database for Global Atmospheric Research, *Sci. Data*, 7, 121, <https://doi.org/10.1038/s41597-020-0462-2>, 2020.
- 705 Eastham, S. D., Long, M. S., Keller, C. A., Lundgren, E., Yantosca, R. M., Zhuang, J., Li, C., Lee, C. J., Yannetti, M., Auer, B. M., Clune, T. L., Kouatchou, J., Putman, W. M., Thompson, M. A., Trayanov, A. L., Molod, A. M., Martin, R. V., and Jacob, D. J.: GEOS-Chem high performance (GCHP v11-02c): A next-generation implementation of the GEOS-Chem chemical transport model for massively parallel applications, *Geosci. Model Dev.*, 11, 2941–2953, <https://doi.org/10.5194/gmd-11-2941-2018>, 2018.
- 710 EU: DIRECTIVE (EU) 2016/2284 OF THE EUROPEAN PARLIAMENT AND OF THE COUNCIL of 14 December 2016 on the reduction of national emissions of certain atmospheric pollutants, amending Directive 2003/35/EC and repealing Directive 2001/81/EC, *Off. J. Eur. Union*, L 344, 1–31, 2016.
- Fu, H., Luo, Z., and Hu, S.: A temporal-spatial analysis and future trends of ammonia emissions in China, *Sci. Total Environ.*, 731, 138897, <https://doi.org/10.1016/j.scitotenv.2020.138897>, 2020.
- 715 Fu, X., Wang, S., Xing, J., Zhang, X., Wang, T., and Hao, J.: Increasing Ammonia Concentrations Reduce the Effectiveness of Particle Pollution Control Achieved via SO<sub>2</sub> and NO<sub>x</sub> Emissions Reduction in East China, *Environ. Sci. Technol. Lett.*, 4, 221–227, <https://doi.org/10.1021/acs.estlett.7b00143>, 2017.

- Gao, Z., Ma, W., Zhu, G., and Roelcke, M.: Estimating farm-gate ammonia emissions from major animal production systems in China, *Atmos. Environ.*, 79, 20–28, <https://doi.org/10.1016/j.atmosenv.2013.06.025>, 2013.
- 720 Gelaro, R., McCarty, W., Suárez, M. J., Todling, R., Molod, A., Takacs, L., Randles, C. A., Darmenov, A., Bosilovich, M. G., Reichle, R., Wargan, K., Coy, L., Cullather, R., Draper, C., Akella, S., Buchard, V., Conaty, A., da Silva, A. M., Gu, W., Kim, G. K., Koster, R., Lucchesi, R., Merkova, D., Nielsen, J. E., Partyka, G., Pawson, S., Putman, W., Rienecker, M., Schubert, S. D., Sienkiewicz, M., and Zhao, B.: The modern-era retrospective analysis for research and applications, version 2 (MERRA-2), *J. Clim.*, 30, 5419–5454, <https://doi.org/10.1175/JCLI-D-16-0758.1>, 2017.
- 725 Groenestein, C. M., Hutchings, N. J., Haenel, H. D., Amon, B., Menzi, H., Mikkelsen, M. H., Misselbrook, T. H., van Bruggen, C., Kupper, T., and Webb, J.: Comparison of ammonia emissions related to nitrogen use efficiency of livestock production in Europe, *J. Clean. Prod.*, 211, 1162–1170, <https://doi.org/10.1016/j.jclepro.2018.11.143>, 2019.
- Gu, B., Ju, X., Chang, J., Ge, Y., and Vitousek, P. M.: Integrated reactive nitrogen budgets and future trends in China, *Proc. Natl. Acad. Sci.*, 112, 8792–8797, <https://doi.org/10.1073/pnas.1510211112>, 2015.
- 730 Gu, B., Ju, X., Chang, S. X., Ge, Y., and Chang, J.: Nitrogen use efficiencies in Chinese agricultural systems and implications for food security and environmental protection, *Reg. Environ. Chang.*, 17, 1217–1227, <https://doi.org/10.1007/s10113-016-1101-5>, 2017.
- Gu, B., Zhang, L., Dingenen, R. Van, Vieno, M., Grinsven, H. J. Van, Zhang, X., Zhang, S., Chen, Y., Wang, S., Ren, C., Rao, S., Holland, M., Winiwarer, W., Chen, D., Xu, J., and Sutton, M. A.: Abating ammonia is more cost-effective than nitrogen oxides for mitigating PM2.5 air pollution, *Science* (80-. ), 374, 758–762, <https://doi.org/10.1126/science.abf8623>, 2021.
- 735 Guo, Y., Chen, Y., Searchinger, T. D., Zhou, M., Pan, D., Yang, J., Wu, L., Cui, Z., Zhang, W., Zhang, F., Ma, L., Sun, Y., Zondlo, M. A., Zhang, L., and Mauzerall, D. L.: Air quality, nitrogen use efficiency and food security in China are improved by cost-effective agricultural nitrogen management, *Nat. Food*, 1, 648–658, <https://doi.org/10.1038/s43016-020-00162-z>, 2020.
- 740 Gyldenkerne, S., Skjøth, C. A., Hertel, O., and Ellermann, T.: A dynamical ammonia emission parameterization for use in air pollution models, *J. Geophys. Res. Atmos.*, 110, 1–14, <https://doi.org/10.1029/2004JD005459>, 2005.
- Han, X., Zhu, L., Liu, M., Song, Y., and Zhang, M.: Numerical analysis of agricultural emissions impacts on PM2.5 in China using a high-resolution ammonia emission inventory, *Atmos. Chem. Phys.*, 20, 9979–9996, <https://doi.org/10.5194/acp-20-9979-2020>, 2020.
- 745 Henze, D. K., Shindell, D. T., Akhtar, F., Spurr, R. J. D., Pinder, R. W., Loughlin, D., Kopacz, M., Singh, K., and Shim, C.: Spatially refined aerosol direct radiative forcing efficiencies, *Environ. Sci. Technol.*, 46, 9511–9518, <https://doi.org/10.1021/es301993s>, 2012.
- Hou, Y., Velthof, G. L., and Oenema, O.: Mitigation of ammonia, nitrous oxide and methane emissions from manure management chains: A meta-analysis and integrated assessment, *Glob. Chang. Biol.*, 21, 1293–1312, <https://doi.org/10.1111/gcb.12767>, 2015.
- 750 Huang, S., Lv, W., Bloszies, S., Shi, Q., Pan, X., and Zeng, Y.: Effects of fertilizer management practices on yield-scaled ammonia emissions from croplands in China: A meta-analysis, *F. Crop. Res.*, 192, 118–125, <https://doi.org/10.1016/j.fcr.2016.04.023>, 2016.
- 755 Huang, X., Song, Y., Li, M., Li, J., Huo, Q., Cai, X., Zhu, T., Hu, M., and Zhang, H.: A high-resolution ammonia emission inventory in China, *Global Biogeochem. Cycles*, 26, 1–14, <https://doi.org/10.1029/2011GB004161>, 2012.
- Jin, X., Zhang, N., Zhao, Z., Bai, Z., and Ma, L.: Nitrogen budgets of contrasting crop-livestock systems in China, *Environ. Pollut.*, 288, 117633, <https://doi.org/10.1016/j.envpol.2021.117633>, 2021.
- 760 Kang, Y., Liu, M., Song, Y., Huang, X., Yao, H., Cai, X., Zhang, H., Kang, L., Liu, X., Yan, X., He, H., Zhang, Q., Shao, M., and Zhu, T.: High-resolution ammonia emissions inventories in China from 1980 to 2012, *Atmos. Chem. Phys.*, 16, 2043–2058, <https://doi.org/10.5194/acp-16-2043-2016>, 2016.

- Kurokawa, J. and Ohara, T.: Long-term historical trends in air pollutant emissions in Asia: Regional Emission inventory in ASia (REAS) version 3, *Atmos. Chem. Phys.*, 20, 12761–12793, <https://doi.org/10.5194/acp-20-12761-2020>, 2020.
- 765 Li, B., Chen, L., Shen, W., Jin, J., Wang, T., Wang, P., Yang, Y., and Liao, H.: Improved gridded ammonia emission inventory in China, *Atmos. Chem. Phys.*, 21, 15883–15900, <https://doi.org/10.5194/acp-21-15883-2021>, 2021.
- Li, M., Liu, H., Geng, G., Hong, C., Liu, F., Song, Y., Tong, D., Zheng, B., Cui, H., Man, H., Zhang, Q., and He, K.: Anthropogenic emission inventories in China: a review, *Natl. Sci. Rev.*, 4, 834–866, <https://doi.org/10.1093/nsr/nwx150>, 2017.
- Liu, H. and Zheng, K.: Analysis of the Chinese government’s subsidy programs to restore the pork supply chain: The case of African swine fever, *Omega (United Kingdom)*, 124, 102995, <https://doi.org/10.1016/j.omega.2023.102995>, 2024.
- 770 Liu, L., Xu, W., Lu, X., Zhong, B., Guo, Y., Lu, X., Zhao, Y., He, W., Wang, S., Zhang, X., Liu, X., and Vitousek, P.: Exploring global changes in agricultural ammonia emissions and their contribution to nitrogen deposition since 1980, *Proc. Natl. Acad. Sci.*, 119, <https://doi.org/10.1073/pnas.2121998119>, 2022a.
- Liu, P., Ding, J., Liu, L., Xu, W., and Liu, X.: Estimation of surface ammonia concentrations and emissions in China from the polar-orbiting Infrared Atmospheric Sounding Interferometer and the FY-4A Geostationary Interferometric Infrared Sounder, *Atmos. Chem. Phys.*, 22, 9099–9110, <https://doi.org/10.5194/acp-22-9099-2022>, 2022b.
- 775 Liu, P., Ding, J., Ji, Y., Xu, H., Liu, S., Xiao, B., Jin, H., Zhong, X., Guo, Z., Wang, H., and Liu, L.: Satellite Support to Estimate Livestock Ammonia Emissions: A Case Study in Hebei, China, *Atmosphere (Basel)*, 13, 1552, <https://doi.org/10.3390/atmos13101552>, 2022c.
- 780 Liu, X., Sha, Z., Song, Y., Dong, H., Pan, Y., Gao, Z., Li, Y., Ma, L., Dong, W., Hu, C., Wang, W., Wang, Y., Geng, H., Zheng, Y., and Gu, M.: China’s Atmospheric Ammonia Emission Characteristics, Mitigation Options and Policy Recommendations, *Res. Environ. Sci.*, 34, 149–157, 2021a.
- Liu, X., Tai, A. P. K., Chen, Y., Zhang, L., Shaddick, G., Yan, X., and Lam, H. M.: Dietary shifts can reduce premature deaths related to particulate matter pollution in China, *Nat. Food*, 2, 997–1004, <https://doi.org/10.1038/s43016-021-00430-6>, 2021b.
- 785 Liu, X., Zhang, D., Wu, H., Elser, J. J., and Yuan, Z.: Uncovering the spatio-temporal dynamics of crop-specific nutrient budgets in China, *J. Environ. Manage.*, 340, 117904, <https://doi.org/10.1016/j.jenvman.2023.117904>, 2023.
- Liu, Z., Zhou, M., Chen, Y., Chen, D., Pan, Y., Song, T., Ji, D., Chen, Q., and Zhang, L.: The nonlinear response of fine particulate matter pollution to ammonia emission reductions in North China, *Environ. Res. Lett.*, 16, <https://doi.org/10.1088/1748-9326/abdf86>, 2021c.
- 790 Luo, Y., Zhang, Z., Li, Z., Chen, Y., Zhang, L., Cao, J., and Tao, F.: Identifying the spatiotemporal changes of annual harvesting areas for three staple crops in China by integrating multi-data sources, *Environ. Res. Lett.*, 15, 074003, <https://doi.org/10.1088/1748-9326/ab80f0>, 2020.
- Martin, R. V., Eastham, S. D., Bindle, L., Lundgren, E. W., Clune, T. L., Keller, C. A., Downs, W., Zhang, D., Lucchesi, R. A., Sulprizio, M. P., Yantosca, R. M., Li, Y., Estrada, L., Putman, W. M., Auer, B. M., Trayanov, A. L., Pawson, S., and Jacob, D. J.: Improved advection, resolution, performance, and community access in the new generation (version 13) of the high-performance GEOS-Chem global atmospheric chemistry model (GCHP), *Geosci. Model Dev.*, 15, 8731–8748, <https://doi.org/10.5194/gmd-15-8731-2022>, 2022.
- 795 McDuffie, E. E., Smith, S. J., O’Rourke, P., Tibrewal, K., Venkataraman, C., Marais, E. A., Zheng, B., Crippa, M., Brauer, M., and Martin, R. V.: A global anthropogenic emission inventory of atmospheric pollutants from sector- And fuel-specific sources (1970–2017): An application of the Community Emissions Data System (CEDS), *Earth Syst. Sci. Data*, 12, 3413–3442, <https://doi.org/10.5194/essd-12-3413-2020>, 2020.
- 800 Meng, W., Zhong, Q., Yun, X., Zhu, X., Huang, T., Shen, H., Chen, Y., Chen, H., Zhou, F., Liu, J., Wang, X., Zeng, E. Y., and Tao, S.: Improvement of a Global High-Resolution Ammonia Emission Inventory for Combustion and Industrial Sources with New Data from the Residential and Transportation Sectors, *Environ. Sci. Technol.*, 51, 2821–2829, <https://doi.org/10.1021/acs.est.6b03694>, 2017.
- 805

- Miao, R., Chen, Q., Zheng, Y., Cheng, X., Sun, Y., Palmer, P. I., Shrivastava, M., Guo, J., Zhang, Q., Liu, Y., Tan, Z., Ma, X., Chen, S., Zeng, L., Lu, K., and Zhang, Y.: Model bias in simulating major chemical components of PM<sub>2.5</sub> in China, *Atmos. Chem. Phys.*, 20, 12265–12284, <https://doi.org/10.5194/acp-20-12265-2020>, 2020.
- 810 National Bureau of Statistics of China: <http://www.stats.gov.cn/english/>, last access: 24 December 2023.
- Pan, Y., Tian, S., Zhao, Y., Zhang, L., Zhu, X., Gao, J., Huang, W., Zhou, Y., Song, Y., Zhang, Q., and Wang, Y.: Identifying Ammonia Hotspots in China Using a National Observation Network, *Environ. Sci. Technol.*, 52, 3926–3934, <https://doi.org/10.1021/acs.est.7b05235>, 2018.
- 815 Paulot, F., Jacob, D. J., Pinder, R. W., Bash, J. O., Travis, K., and Henze, D. K.: Ammonia emissions in the United States, European Union, and China derived by high-resolution inversion of ammonium wet deposition data: Interpretation with a new agricultural emissions inventory (MASAGE\_NH<sub>3</sub>), *J. Geophys. Res.*, 119, 4343–4364, <https://doi.org/10.1002/2013JD021130>, 2014.
- Peng, S., Ding, Y., Liu, W., and Li, Z.: 1 km monthly temperature and precipitation dataset for China from 1901 to 2017, *Earth Syst. Sci. Data*, 11, 1931–1946, <https://doi.org/10.5194/essd-11-1931-2019>, 2019.
- 820 Ren, K., Xu, M., Li, R., Zheng, L., Liu, S., Reis, S., Wang, H., Lu, C., Zhang, W., Gao, H., Duan, Y., and Gu, B.: Optimizing nitrogen fertilizer use for more grain and less pollution, *J. Clean. Prod.*, 360, 132180, <https://doi.org/10.1016/j.jclepro.2022.132180>, 2022.
- Sacks, W. J., Deryng, D., Foley, J. A., and Ramankutty, N.: Crop planting dates: An analysis of global patterns, *Glob. Ecol. Biogeogr.*, 19, 607–620, <https://doi.org/10.1111/j.1466-8238.2010.00551.x>, 2010.
- 825 Song, Q., Chen, Y., Zhao, L., Ouyang, H., and Song, J.: Monitoring of sausage products sold in Sichuan Province, China: a first comprehensive report on meat species' authenticity determination, *Sci. Rep.*, 9, 19074, <https://doi.org/10.1038/s41598-019-55612-x>, 2019.
- Sutton, M. A., Howard, C. M., Mason, K. E., Brownlie, W. J., and Cordovil, D. S.: Nitrogen Opportunities for Agriculture, Food & Environment UNECE Guidance Document on Integrated, 2022.
- 830 Wang, C., Cheng, K., Ren, C., Liu, H., Sun, J., Reis, S., Yin, S., Xu, J., and Gu, B.: An empirical model to estimate ammonia emission from cropland fertilization in China, *Environ. Pollut.*, 288, 117982, <https://doi.org/10.1016/j.envpol.2021.117982>, 2021.
- Wang, X., Bai, X., Zhu, Z. C., Zhou, P., Miao, P., Hen, and Zhou, J.: Nitrogen Use and Management in Orchards and Vegetable Fields in China: Challenges and Solutions, *Front. Agric. Sci. Eng.*, 9, 386–395, <https://doi.org/10.15302/J-FASE-2022443>, 2022a.
- 835 Wang, X., Bai, X., Zhu, Z. C., Zhou, P., Miao, P., Hen, and Zhou, J.: Nitrogen Use and Management in Orchards and Vegetable Fields in China: Challenges and Solutions, *Front. Agric. Sci. Eng.*, 9, 386–395, <https://doi.org/10.15302/J-FASE-2022443>, 2022b.
- Whitnall, T. and Pitts, N.: Global trends in meat consumption, *ABARES Agric. Commod.*, 96–99, 2019.
- 840 Xie, P. and Liao, H.: The Impacts of Changes in Anthropogenic Emissions Over China on PM<sub>2.5</sub> Concentrations in South Korea and Japan During 2013–2017, *Front. Environ. Sci.*, 10, <https://doi.org/10.3389/fenvs.2022.841285>, 2022.
- Xu, P., Zhang, Y., Gong, W., Hou, X., Kroeze, C., Gao, W., and Luan, S.: An inventory of the emission of ammonia from agricultural fertilizer application in China for 2010 and its high-resolution spatial distribution, *Atmos. Environ.*, 115, 141–148, <https://doi.org/10.1016/j.atmosenv.2015.05.020>, 2015.
- 845 Xu, W., Zhao, Y., Wen, Z., Chang, Y., Pan, Y., Sun, Y., Ma, X., Sha, Z., Li, Z., Kang, J., Liu, L., Tang, A., Wang, K., Zhang, Y., Guo, Y., Zhang, L., Sheng, L., Zhang, X., Gu, B., Song, Y., Van Damme, M., Clarisse, L., Coheur, P.-F., Collett, J. L., Goulding, K., Zhang, F., He, K., and Liu, X.: Increasing importance of ammonia emission abatement in PM<sub>2.5</sub> pollution control, *Sci. Bull.*, 67, 1745–1749, <https://doi.org/10.1016/j.scib.2022.07.021>, 2022.
- Yang, Y., Liu, L., Liu, P., Ding, J., Xu, H., and Liu, S.: Improved global agricultural crop- and animal-specific ammonia emissions during 1961–2018, *Agric. Ecosyst. Environ.*, 344, 108289, <https://doi.org/10.1016/j.agee.2022.108289>, 2023.
- 850



- Ye, Z., Guo, X., Cheng, L., Cheng, S., Chen, D., Wang, W., and Liu, B.: Reducing PM<sub>2.5</sub> and secondary inorganic aerosols by agricultural ammonia emission mitigation within the Beijing-Tianjin-Hebei region, China, *Atmos. Environ.*, 219, 116989, <https://doi.org/10.1016/j.atmosenv.2019.116989>, 2019.
- 855 Yu, Z., Liu, J., and Kattel, G.: Historical nitrogen fertilizer use in China from 1952 to 2018, *Earth Syst. Sci. Data*, 14, 5179–5194, <https://doi.org/10.5194/essd-14-5179-2022>, 2022.
- Zhai, S., Jacob, D. J., Brewer, J. F., Li, K., Moch, J. M., Kim, J., Lee, S., Lim, H., Lee, H. C., Kuk, S. K., Park, R. J., Jeong, J. I., Wang, X., Liu, P., Luo, G., Yu, F., Meng, J., Martin, R. V., Travis, K. R., Hair, J. W., Anderson, B. E., Dibb, J. E., Jimenez, J. L., Campuzano-Jost, P., Nault, B. A., Woo, J. H., Kim, Y., Zhang, Q., and Liao, H.: Relating geostationary satellite measurements of aerosol optical depth (AOD) over East Asia to fine particulate matter (PM<sub>2.5</sub>): insights from the
- 860 KORUS-AQ aircraft campaign and GEOS-Chem model simulations, *Atmos. Chem. Phys.*, 21, 16775–16791, <https://doi.org/10.5194/acp-21-16775-2021>, 2021.
- Zhan, X., Adalibieke, W., Cui, X., Winiwarter, W., Reis, S., Zhang, L., Bai, Z., Wang, Q., Huang, W., and Zhou, F.: Improved Estimates of Ammonia Emissions from Global Croplands, *Environ. Sci. Technol.*, 55, 1329–1338, <https://doi.org/10.1021/acs.est.0c05149>, 2021.
- 865 Zhang, L., Chen, Y., Zhao, Y., Henze, D. K., Zhu, L., Song, Y., Paulot, F., Liu, X., Pan, Y., Lin, Y., and Huang, B.: Agricultural ammonia emissions in China: Reconciling bottom-up and top-down estimates, *Atmos. Chem. Phys.*, 18, 339–355, <https://doi.org/10.5194/acp-18-339-2018>, 2018.
- Zhang, Q.: Nitrogen, phosphorus and potassium nutrient balance and optimization approaches of major crops in China, China Agricultural University, 2021.
- 870 Zhang, Q., Chu, Y., Yin, Y., Ying, H., Zhang, F., and Cui, Z.: Comprehensive assessment of the utilization of manure in China's croplands based on national farmer survey data, *Sci. Data*, 10, 223, <https://doi.org/10.1038/s41597-023-02154-7>, 2023.
- Zhang, X., Wu, Y., Liu, X., Reis, S., Jin, J., Dragosits, U., Van Damme, M., Clarisse, L., Whitburn, S., Coheur, P.-F., and Gu, B.: Ammonia Emissions May Be Substantially Underestimated in China, *Environ. Sci. Technol.*, 51, 12089–12096, <https://doi.org/10.1021/acs.est.7b02171>, 2017.
- 875 Zhang, X., Gu, B., van Grinsven, H., Lam, S. K., Liang, X., Bai, M., and Chen, D.: Societal benefits of halving agricultural ammonia emissions in China far exceed the abatement costs, *Nat. Commun.*, 11, 4357, <https://doi.org/10.1038/s41467-020-18196-z>, 2020a.
- Zhang, X., Gu, B., van Grinsven, H., Lam, S. K., Liang, X., Bai, M., and Chen, D.: Societal benefits of halving agricultural ammonia emissions in China far exceed the abatement costs, *Nat. Commun.*, 11, <https://doi.org/10.1038/s41467-020-18196-z>, 2020b.
- 880 Zhang, X., Zou, T., Lassaletta, L., Mueller, N. D., Tubiello, F. N., Lisk, M. D., Lu, C., Conant, R. T., Dorich, C. D., Gerber, J., Tian, H., Bruulsema, T., Maaz, T. M. C., Nishina, K., Bodirsky, B. L., Popp, A., Bouwman, L., Beusen, A., Chang, J., Havlik, P., Leclère, D., Canadell, J. G., Jackson, R. B., Heffer, P., Wanner, N., Zhang, W., and Davidson, E. A.: Quantification of global and national nitrogen budgets for crop production, *Nat. Food*, 2, 529–540, <https://doi.org/10.1038/s43016-021-00318-5>, 2021a.
- Zhang, X., Ren, C., Gu, B., and Chen, D.: Uncertainty of nitrogen budget in China, *Environ. Pollut.*, 286, 117216, <https://doi.org/10.1016/j.envpol.2021.117216>, 2021b.
- 890 Zhao, Y. G., Gordon, A. W., O'Connell, N. E., and Yan, T.: Nitrogen utilization efficiency and prediction of nitrogen excretion in sheep offered fresh perennial ryegrass (*Lolium perenne*), *J. Anim. Sci.*, 94, 5321–5331, <https://doi.org/10.2527/jas.2016-0541>, 2016.